NOTICE

THE ATTACHED FILES ARE OFFICIAL RECORDS OF THE OFFICE OF REGULATION. THEY HAVE BEEN CHARGED TO YOU FOR A LIMITED TIME PERIOD ANS MUST BE RETURNED TO THE CENTRAL RECORDS STATION 008. ANY PAGE(S) REMOVED FOR REPRODUCTION MUST BE RETURNED TO ITS/THEIR ORIGINAL ORDER.

DEADLINE RETURN DATE 50-237/249/254/265

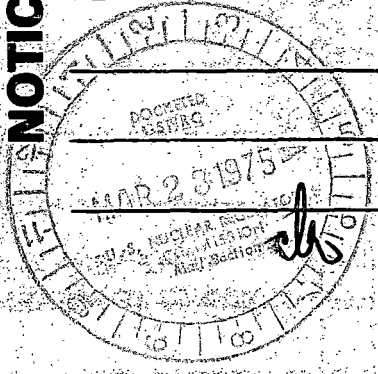

Recd w/ltr dtd 3-18-75

MARY JINKS, CHIEF
CENTRAL RECORDS STATION

3415

NOTICE

DRESDEN STATION SPECIAL REPORT NO. 39

QUAD-CITIES STATION SPECIAL REPORT NO. 14

ANALYSIS OF HYDROGEN GENERATION AND
CONTROL IN PRIMARY CONTAINMENT FOLLOWING
POSTULATED LOSS OF COOLANT ACCIDENT

FOR

DRESDEN UNITS 2 AND 3 AND QUAD-CITIES UNITS 1 AND 2

PREPARED BY
ENERGY INCORPORATED

DRESDEN STATION SPECIAL REPORT NO. 39

QUAD-CITIES STATION SPECIAL REPORT NO. 14

ANALYSIS OF HYDROGEN GENERATION AND CONTROL IN PRIMARY CONTAINMENT FOLLOWING POSTULATED LOSS OF COOLANT ACCIDENT

FOR

DRESDEN UNITS 2 AND 3 AND QUAD-CITIES UNITS 1 AND 2

PREPARED BY
ENERGY INCORPORATED
December 1974

TABLE OF CONTENTS

TABLE OF CONTENTS (Cont'd.)

TABLES

FIGURES

FIGURES (Cont'd.)

ABSTRACT

A study was performed with the objective of reviewing the control of combustible gas concentrations in containments following a postulated loss-of-coolant accident (LOCA) for Commonwealth Edison's operating Boiling Water Reactors (BWR's). This study included an extensive review and appraisal of the provisions of both the April 5, 1974 draft[1] and the August 14, 1974 draft[2] of Regulatory Guide 1.7. In addition, this study included analyses using the acceptable methods described in the August 14, 1974 draft of Regulatory Guide 1.7 for conservatively calculating the metal-water reaction-generated hydrogen and the containment hydrogen concentration following a hypothetical LOCA. The conservative calculation of the metal-water reaction, using 10 CFR 50.46[3], showed that the maximum percentage of mass of cladding surrounding the fuel that reacts with water is less than 0.1 percent for both the Dresden and the Quad-Cities Units. Since the August 14, 1974 draft of Regulatory Guide 1.7 specifies the minimum amount of core-wide cladding involved in metal-water reaction and this specified minimum amount (0.72%) exceeds five times the maximum calculated (0.5%), an analysis of the containment hydrogen buildup following a postulated LOCA was performed using this specified minimum amount and all other assumptions delineated in the August 14, 1974 draft of Regulatory Guide 1.7.

For the above analysis, an atmospheric containment atmosphere dilution system (ACADS) was used to control the containment hydrogen concentration to below four-volume percent (4 v/o). Periodic purging was used to control the containment pressure. The calculated radiological consequences from purging the containment combined with the conservative radiological consequence, calculated by the Staff in their safety evaluations for the Dresden and the Quad-City Units, for a hypothetical LOCA resulted in total biological doses below the 10 CFR 100[4] requirements.

In view of the conservatisms inherent in the calculations for the metal-water reaction-generated hydrogen during a hypothetical LOCA, the additional safety margins in the 4 v/o containment hydrogen concentration limit,

and the safety margin existing in the total radiological dose resulting from purging plus LOCA, it was concluded that the requirement for containment inerting has no sound technical basis and should be removed from the Dresden and the Quad-Cities technical specifications.

I. INTRODUCTION

Because of concerns of the power generating industry and the general belief that containment inerting is inconsistent with the dual goals of maximum public safety and reliable nuclear power, Commonwealth Edison along with a group of five other utility companies* in December, 1971 entered into an agreement with Rockwell International Corporation (Atomics International Division) to carry out an independent experimental program for determination of flammability limits and detonation initiation of hydrogen-air-water spray mixtures in a simulated post-LOCA reactor containment environment. A final report[5] was issued on May 11, 1973. The Atomics International (AI) studies generally confirm and augment the recent work of General Electric[6] and others.[7] These AI studies also show that the containment water spray is effective in causing gas mixing and in greatly suppressing the temperature and pressure rises caused by flammation or detonation. Flammation is the special case of combustion in which the flame propagates through a mixture of gases. In addition, the spray caused a small increase in the lower flammability limit (i.e., an increase in hydrogen concentration before ignition occurs). The AI data indicates modest pressure rises from burning hydrogen-air mixtures up to 12 percent hydrogen. With the addition of water spray, typical of sprays in BWR drywells, containment pressures were very well suppressed. Peak pressures were less than twice the initial pressures for 12 percent hydrogen-air mixtures and only slightly more than double for 16 percent hydrogen air mixtures.

With these encouraging results, showing that the containment sprays provide an additional safety margin against hydrogen burning in the containment, Commonwealth Edison elected to perform a detailed review of the control of combustible gas concentrations in BWR containments following a postulated LOCA. Such a review seemed particularly appropriate in

---

*Other utility companies were Boston Edison Company, Detroit Edison Company, Philadelphia Electric Company, Public Service Electric & Gas Company, and Yankee Atomic Electric Company.

view of the new 10 CFR 50.46 ECCS Criteria and the recently issued April 5, 1974 revision of Regulatory Guide 1.7. Furthermore, the possibility existed that an analysis for the Quad-Cities and Dresden Units could have broader implications for the whole industry in terms of the containment inerting question and therefore would be a logical extension to the AI flammability studies.

Accordingly, the approach taken was to study the complete accident sequence following a hypothetical LOCA and to perform the following calculations:

1) Percent metal-water reaction (MWR) and hydrogen release calculated using the new 10 CFR 50.46 ECCS criteria.

2) Resulting containment hydrogen concentration (volume percent versus time).

3) Radiological impact (thyroid doses) from the operation of the atmospheric containment atmosphere dilution system (ACADS) for post-LOCA hydrogen control.

4) Review of hydrogen flammability data with and without water sprays.

Commonwealth Edison contracted with Energy Incorporated (EI) to perform the above outlined analysis and the results of this analsysis are contained in the first draft of the Dresden Station Special Report No. 39 and Quad-Cities Station Special Report No. 14.

The analysis presented in the above draft report justified further changes in the April 5, 1974 draft of Regulatory Guide 1.7.

Subsequently, a draft of Regulatory Guide 1.7 was issued August 14, 1974. This draft retained the guideline of five times the maximum calculated metal-water reaction under 10 CFR 50.46 but replaced the requirement of 1 percent metal-water reaction with a guideline for a minimum metal-water reaction

assumption. More specifically, the amount of hydrogen assumed to be generated by metal-water reaction should be five times the maximum amount calculated under 10 CFR 50.46, but no less than the amount that would result from a core-wide reaction of all the metal on the outside surfaces of the cladding surrounding the fuel, to a depth of 0.00023 inches. Thus, for a BWR with 7 X 7 fuel assemblies having a cladding thickness of 0.032 inches, a 0.00023 inch penetration represents a 0.72 percent metal-water reaction. This assumption of a minimum metal-water reaction (0.72%) is greater than five times the maximum metal-water reaction calculated under 10 CFR 50.46 (0.5%) for both the Dresden and the Quad-Cities units. Therefore, a re-evaluation of the hydrogen buildup in the containments of the two stations following a postulated LOCA was deemed necessary.

Commonwealth Edison contracted with Energy Incorporated to perform this re-evaluation and to incorporate the results of this analysis into the first draft of the Dresden Station Special Report No. 39 and the Quad-Cities Station Special Report No. 14.

The approach taken for this analysis was to study the complete accident sequence following a hypothetical LOCA and to perform the following calculations:

1) Percent metal-water reaction and hydrogen release calculated using the new 10 CFR 50.46 criteria to ascertain that five times the maximum calculated metal-water reaction under 10 CFR 50.46 is less than 0.72 percent.

2) Percent metal-water reaction and hydrogen release calculated using the assumption of a minimum metal-water reaction specified in the August 14, 1974 draft of Regulatory Guide 1.7.

3) The resulting maximum containment hydrogen concentration (volume percent vs. time) as calculated under items 1 or 2.

4) Radiological impact (thyroid doses) from the operation of the atmospheric containment atmosphere dilution system (ACADS) for post-LOCA hydrogen control.

One of the difficulties in performing the metal-water reaction calculation is that at the time of this analysis there were no approved analytical models for calculating metal-water reaction using the new 10 CFR 50.46 criteria. However, the analytical models presented herein, for calculating the metal-water reaction during a postulated LOCA, interpret the new criteria conservatively and therefore give an acceptable estimate of the metal-water reaction-generated hydrogen.

II. UTILITY OPERATING EXPERIENCE WITH INERTED CONTAINMENTS

Commonwealth Edison has been strongly opposed to nitrogen inerting of BWR primary containments since the issue was raised during the licensing proceedings of the Dresden Units 2 and 3. The reasons for this opposition to containment inerting were expressed at some length in both Amendment 23 of the Dresden FSAR[8] and during the ACRS review of Dresden Unit 2. These same reasons have been reiterated by a number of other utilities throughout the country during their licensing proceedings.

As of June, 1974, Commonwealth Edison has accumulated 8.5 reactor years of operating experience on the Dresden 2 and 3 and Quad-Cities 1 and 2 Units with the primary containment nitrogen inerted. By the use of strict operating procedures and through good judgment on the part of the stations' operating staff, fortunately there has not been any injury to personnel entering the containment such as has occurred due to inerted containments at other commercial reactor sites. In addition, although it must be done during shutdown, Commonwealth Edison has been able to make the necessary inspections of primary system components (pumps, valves, pipe snubbers, etc.) to assure the continued safe operation of these nuclear power units. However, Commonwealth Edison's experience has confirmed the earlier assessment of inerting; namely, that it is an operational nuisance which poses a finite and real danger to operating personnel and militates against timely inspections of important and safety related reactor components. In addition, as a result of experience, Commonwealth Edison has identified the following additional undesirable facets of BWR containment inerting:

1) The requirement to maintain the oxygen concentration below a certain value increases the amount of containment venting required and thus increases the amount of radioactive gaseous effluent and, hence, the offsite biological doses. These additional biological doses result from an average of 15 complete purges/year per station for containment entry and approximately 200 ventings/year per station to reduce the oxygen concentration below the limit set in the technical specification.

2) There is a reduction in unit availability because of the delays in startup and shutdown associated with inerting and deinerting. Commonwealth Edison has identified 70 reactor hours and 40 reactor hours of increased outages at the Dresden and Quad-Cities Stations, respectively, for 1973, corresponding to up to 1 percent in availability loss.

3) There is an additional annual operating cost for the two stations of approximately $54,000/year for 21,000,000 SCFM of nitrogen used.

It is clear from past discussions with the Regulatory Staff that the risks to personnel as well as the drawbacks of the very limited access of the reactor equipment in the containment are hard to qualify. However, in the judgment of the utilities listed above, the key to safe plant operation is a program of surveillance. To provide the utmost assurance of safety, it is desirable to have relatively free access to equipment located within the reactor containment. With inerting, entry into the containment becomes a major operation with respect to time and manpower, and a significant risk of asphyxiation exists during initial entry even though the containment must be purged prior to entry. The opinion of all the above listed utilities is that safer operating conditions exist without inerting and this opinion is strongly influenced by the belief that there is no sound technical basis for inerting because, as the following sections show, more than adequate design margins exist without inerting the containment. Therefore, the positive safety aspects offered by unrestricted containment access far outweigh any advantages afforded by containment inerting.

III. CONTAINMENT HYDROGEN CONCENTRATION FOLLOWING A HYPOTHETICAL LOCA

The following discussion applies to the Dresden 2 and 3 and Quad Cities 1 and 2 units, since these plants are virtually identical except for some dissimilarities in the reactor water clean up systems (RWCUS). This results in a net power for the Dresden Units about 0.67 percent higher than that for the Quad-Cities units. It was judged unnecessary to perform the following analyses twice because of this slight difference. The analyses performed were based on the Quad-Cities units due to a better availability of data, however, the conclusions apply equally to all four units.

1.0 SOURCES OF HYDROGEN

1.1 Metal-Water Reaction-Generated Hydrogen

The generation of hydrogen by metal-water reaction between the steam and the zircaloy cladding surrounding the reactor fuel is the single most important source of hydrogen in the containment during the postulated LOCA. The calculation of the metal-water reaction-generated hydrogen was performed in accordance with 10 CFR 50.46 as required by the August 14, 1974 draft of Regulatory Guide 1.7.

1.1.1 Models for Calculating Metal-Water Reaction

The calculation of metal-water reaction-generated hydrogen was separated into two separate parts. The first part of this analysis was to calculate the heat transfer associated with the fuel rod surface during the reactor blowdown period. This calculation was performed in accordance with the requirement of the 10 CFR 50.46 acceptance criteria using a modified version of the code, RELAP4.[9] The calculation included a hot channel calculation to represent those portions of the core where the highest peak power is generated as well as an average core calculation to represent the remaining bundles in the core.

The second part of this analysis included the calculation of the core heat-up and the subsequent hydrogen generation due to metal-water reaction utilizing a version of the code MOXY,[10] MOXEI.[11] Separation of the core into various axial and radial regions allowed a realistic calculation to be performed according to 10 CFR 50.46 for light water-cooled nuclear power reactors. A conservative calculation of the core peak temperature was assured by the utilization of all of the conservative assumptions contained in 10 CFR 50.46. In addition, the heat transfer for the remaining portions of the core was also calculated conservatively by including the requirements of 10 CFR 50.46. Separation of the core into axial and radial regions allows the code MOXEI to perform a fairly precise calculation of the hydrogen generation due to the metal-water reaction. The MWR calculation always assumed that the reaction follows the parabolic rate law of Baker-Just.

The design basis accident considered for this calculation was a typical double ended rupture of the inlet side of the recirculation line. Additionally, rod ballooning and the double metal-water reaction, due to metal-water reaction associated with the bursting of the fuel rod cladding on both the outside as well as the inside of the cladding, have been assumed. Conservative assumptions regarding both the internal fuel rod pressures and the amount of fuel rod ballooning were used so that the calculation can be considered conservative without a great deal of detail being utilized in the analysis model. Appendix A provides a description of both models.

1.1.1.1 Changes to Standard RELAP4

The blowdown calculation was based on a modified version of the recently released RELAP4 code. The changes made to the RELAP4 code were based on the changes required under the new licensing criteria. RELAP4 was chosen as the primary blowdown code calculational vehicle since it encompassed many of the required analysis techniques which are included in 10 CFR 50.46.

The specific changes made to the basic RELAP4 code are defined in the following sections. To begin, the decay of the actinides was included in the reactor physics calculation. This included neptunium and plutonium as well as the isotopes of uranium. In addition, the heat generation rate from the decay of fission products was assumed to be 1.2 times the infinite operating time values proposed in the ANS Standard. The locally generated gamma heat was considered to be totally deposited in the fuel.

Another change in the basic RELAP4 code was the specification that no return to nucleate boiling was allowed once dryout had occurred with the heat transfer mode based on the GE transient CHF correlation. Also, no return to transition boiling heat transfer was allowed once the clad superheat exceeded 300°F.

RELAP4 was also modified to allow the recirculation pump head to vary linearly with the suction fluid quality, with the pump head decreasing to zero for a quality of 1 percent. Since the requirements on fuel cladding rupture and ballooning were included in the core heat-up calculation, no additional changes in RELAP4 were necessary to allow it to meet the new rule for boiling water reactor systems. The additional effects of fuel rod ballooning, double metal-water reaction, and the associated hydrogen generation that were calculated during the core heat-up phase were performed with MOXEI. These modifications and the core heat-up calculation are described in subsequent sections.

1.1.1.2 Changes to Standard MOXY

As stated, the core heat-up calculation was performed with MOXEI, a modified version of MOXY. The development of MOXY was funded by the AEC and has been used by the Regulatory Staff in licensing assessments under the old interim acceptance criteria. The computer code MOXY also served as a parent code for the development of the code 6KILER.[12] The computer code 6KILER is used for the core heat-up calculations of an 8 X 8 array of the standard BWR/6 fuel bundle. The modifications to the code MOXY did not include any changes in the heat conduction equation or the basic

equations associated with the radiation heat transfer matrix. However, the changes which were made allow the code to calculate simulated rod ballooning and the double metal-water reaction to account for the formation of zirc oxide on both the inside and outside surfaces of the clad after the rod had ballooned and ruptured. In addition, a variable gap conductance model was included in the code MOXEI in order to allow for changes in gap conductance for the area associated with fuel rod ballooning. In addition, a hydrogen generation calculation was performed based on the amount of zirc reacted due to the metal-water reaction.

The rod ballooning model contained in the code MOXEI was chosen for its conservative assumptions. A relatively straightforward ballooning model was utilized in which a temperature of 1600°F was chosen as the temperature at which a fuel rod simultaneously ballooned and ruptured. Choice of the 1600°F rupture temperature was made on the fact that more than 90 percent of the fuel rods in a General Electric 7 X 7 fuel rod array have an internal pressure of 200 psi or less for a typical core lifetime. Data[13] showing the fuel rod internal pressure distribution in a BWR core at the end of an equilibrium cycle are shown in Figure III-1. Figure III-2 shows that the the 200 psi fuel rod internal pressure selected from the data shown in Figure III-1 and the 1600°F rupture temperature is conservative. That is, Figure III-2 shows that a rupture temperature of 1600°F is conservative for all internal pressures up to 800 psi. The percent of bundle flow blockage chosen was based primarily on the results obtained from BWR-FLECHT Test ZR-2.[13] Other data from Oak Ridge[14] also substantiated the following model. Clad ballooning at low internal pressures has been found to reduce the coolant cross-sectional flow area from 40 to 60 percent. The results from the FLECHT[13] tests with internally pressurized heater rods show a reduction in coolant cross-sectional flow area of approximately 40 percent over the entire bundle cross-section and in the worst case 60 percent around a single rod. For this calculation, the flow blockage caused by each rod ballooning was conservatively considered to be 70 percent.

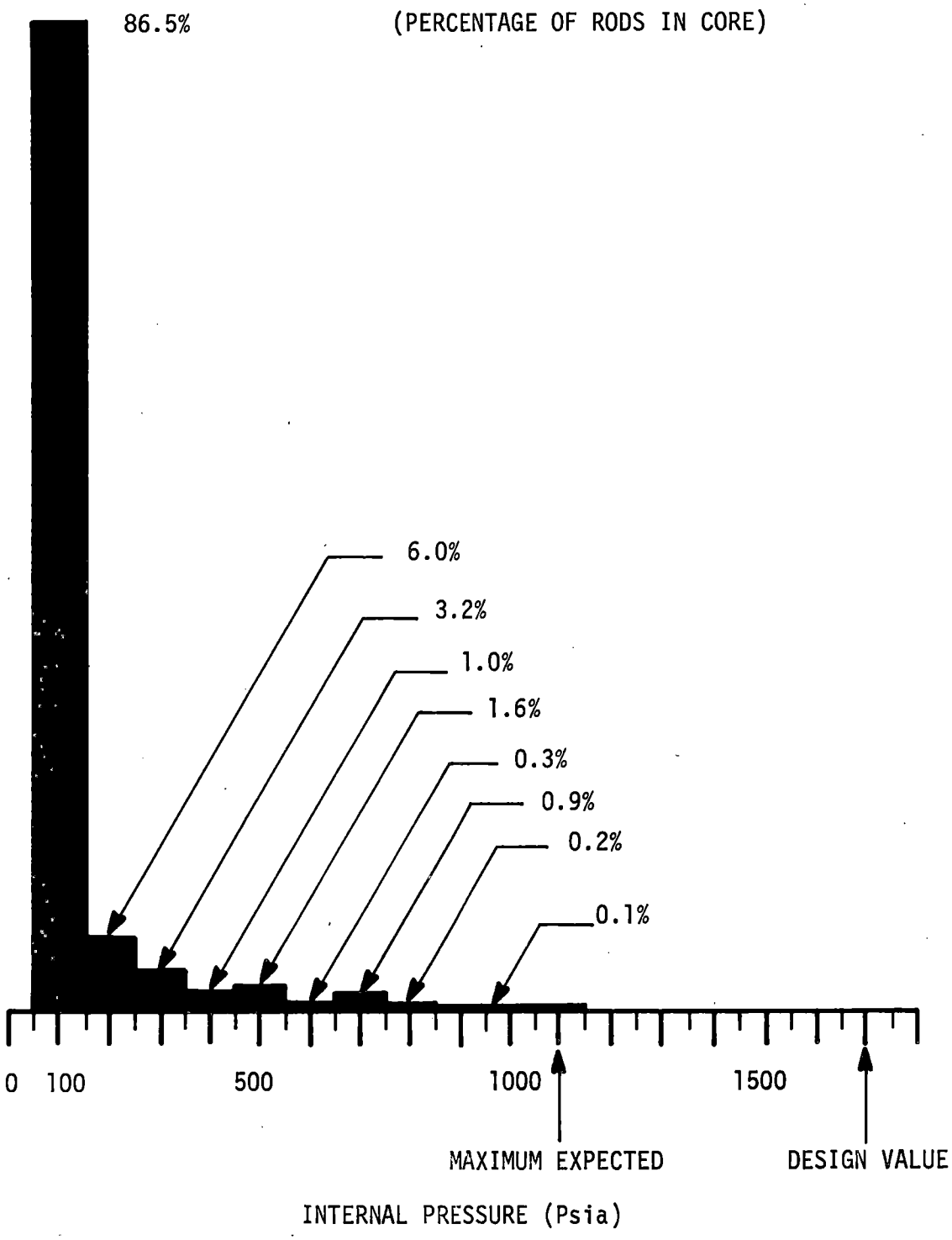

FIGURE III-1 - FUEL ROD INTERNAL PRESSURE DISTRIBUTION IN A BWR CORE AT THE END OF AN EQUILIBRIUM CYCLE (FROM GEAP-13112)[13]

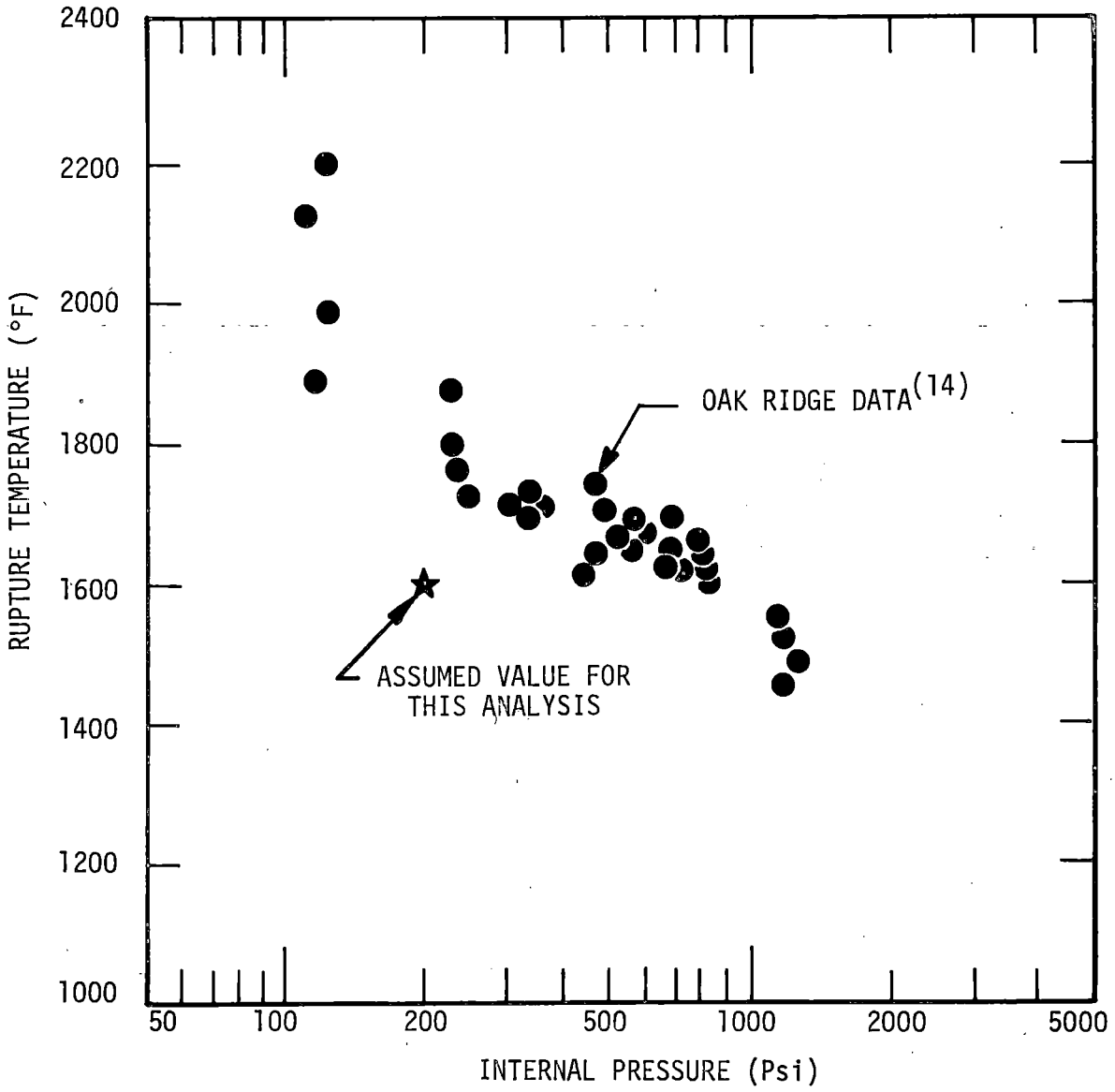

FIGURE III-2 - RUPTURE TEMPERATURE DATA FOR ZIRCALOY CLADDING AS A FUNCTION OF INTERNAL PRESSURE

The sequence of events for the rod ballooning model began with a check on the cladding surface temperature of each rod. For those rods with a cladding surface temperature of 1600°F or greater during any given time step, the code changed the geometry of that particular rod to the specified ballooned geometry which resulted in a flow blockage of 70 percent. A 70 percent flow blockage for all ballooned rods is somewhat synthetic since the flow blockage resulting from a rod which would balloon to touch another rod at a given elevation would result in a flow blockage of 56 percent. Thus, the maximum flow blockage was allowed for the sole purpose of calculating the maximum possible metal-water reaction.

At the time the rod was postulated to simultaneously balloon and rupture the code distributed the existing oxide layer on the outer surface of the rod in equal proportion to the ballooned surface of the rod. That is, the total amount of oxide previously generated on the rod surface before ballooning was distributed on the ballooned surface of the rod in a uniform thickness layer. The metal-water reaction on the inside surface of the rod was assumed to start at the time of ballooning. Thus, the source term for metal-water reaction was the full Baker-Just equation and accounted for time at temperature. All of the energy generated by metal-water reaction was assumed to be deposited within the clad.

At the time of rod ballooning initiation, the code MOXEI changes the specified minimum gap conductance value to a gap conductance dependent on the clad surface temperature, the fuel pellet surface temperature, and the thermal conductivity of the gas within the gap. Thus, after rod ballooning, a gap conductance was computed at each time step based on the temperatures of the fuel pin during the previous time step. The equation for the determination of the gap coefficient include both the radiation heat transfer and the conduction heat transfer modes.

The hydrogen generation as a result of the metal-water reaction was based on the amount of zircaloy reacted due to the zirc-water reaction term. Thus, for every mole of zirc reacted, two moles of hydrogen were

generated. To calculate the total amount of hydrogen generated, the hydrogen generated by the metal-water reaction on each rod was summed to represent the hydrogen generated by the whole bundle at that elevation. In this fashion, it is possible to calculate the hydrogen generation as a function of time and the total accumulated hydrogen generation in the core. Both the rate of hydrogen generation and the total hydrogen accumulation were known at all times during the calculated transient.

Since the rod ballooning within the rod bundle would force a change in the radiation heat transfer, the code was modified to handle this change in a conservative fashion. For the modified radiation heat transfer solution, the rod geometry was assumed to be different from the rod geometry assumed for the double metal-water reaction calculation. The rods were assumed to balloon such that they closed any direct radiation heat transfer beyond those rods directly adjacent to the subject rod.

An internal counter within the code counted the number of rods that were assumed to be ballooned. When ten rods had ballooned, this corresponds to 20 percent of the fuel rod array in the ballooned configuration, the entire rod array viewfactor matrix was assumed to be in a ballooned configuration. Thus, after ten rods had ballooned, only the outer course of rods could radiate directly to the canister surrounding the rod bundle. This geometric representation of the bundle is quite conservative with respect to the radiation heat transfer within the rod bundle.

1.1.2 Results of RELAP4 and MOXEI Calculations

Calculational results from the modified RELAP4 code and the core heat-up code, MOXEI, are presented in the following sections. These calculations meet the requirements of 10 CFR 50.46 and are presented to demonstrate methodology and results for determination of hydrogen generation for a licensing calculational analysis.

1.1.2.1 RELAP4 Results

The initial conditions prior to the recirculation line break were adjusted throughout the system to simulate 102 percent of nominal power (2561 Mw(t)). Three valves were used to simulate a double ended break in one of the recirculating lines, a full pipe area (3.667 ft^2) was opened to the drywell through two valves from each of the two pipe volumes describing the pump suction side. The original unbroken flow path between these two valves was fully blocked by the simultaneous closing of the third valve at the time of the break initiation. The initial pressures and flow distributions are listed in Table III-I. For conservatism, the active bundle flow was assumed to be the minimum value of 0.1113×10^6 lb/hr quoted in NEDO-10299[15] for the hot bundle flow. This assumption maximizes the bypass flow and minimizes the active core flow.

In addition, the power to the recirculation pumps and the feedwater pump was assumed to fail at the time of break initiation. The recirculation pumps were then allowed to coast in response to the fluid flow. Scram initiation occurred at 1.0 second after the break with an additional 0.2 second delay. The 1.0 second initiation time is a conservative estimate for the generation of the high drywell pressure rise of 2 psi required for the scram signal. The resultant power decay curve is shown in Figure III-3.

For the transient, it was assumed that the steamline isolation valves closed in 3.0 seconds after a delay of 0.5 second and the feedwater supply was allowed to coast down in 2.0 seconds.

For the purpose of this calculation, the blowdown transient was calculated from blowdown initiation through the time at which the upper plenum pressure activates the core spray system (350 psig) until full flow of the core spray system. Core spray initiation occurred at 35 seconds in the blowdown transient. Since the core spray valves require 10 seconds to fully open, the core spray was assumed to reach full flow at 45 seconds. This sequence of events is shown in Figure III-4. No credit

TABLE III-I

INITIAL RELAP4 PRESSURE

AND FLOW DISTRIBUTIONS FOR QUAD-CITIES

Power = 2561.22 MWt

Location	Pressure (psia)	Differential Pressure (psid)	Flow (lb/hr)
Core Average	1032.6		8.047×10^7
Core Outlet Plenum	1028.1		9.8×10^7
Steam Dome	1017.4		9.94×10^6
Downcomer	1024.8		9.8×10^7
Lower Plenum	1052.0		9.8×10^7
Recirculation Pump		186.5	1.747×10^7
Hot Bundle	1032.6		0.111×10^6
Core Bypass	1034.2		1.742×10^7

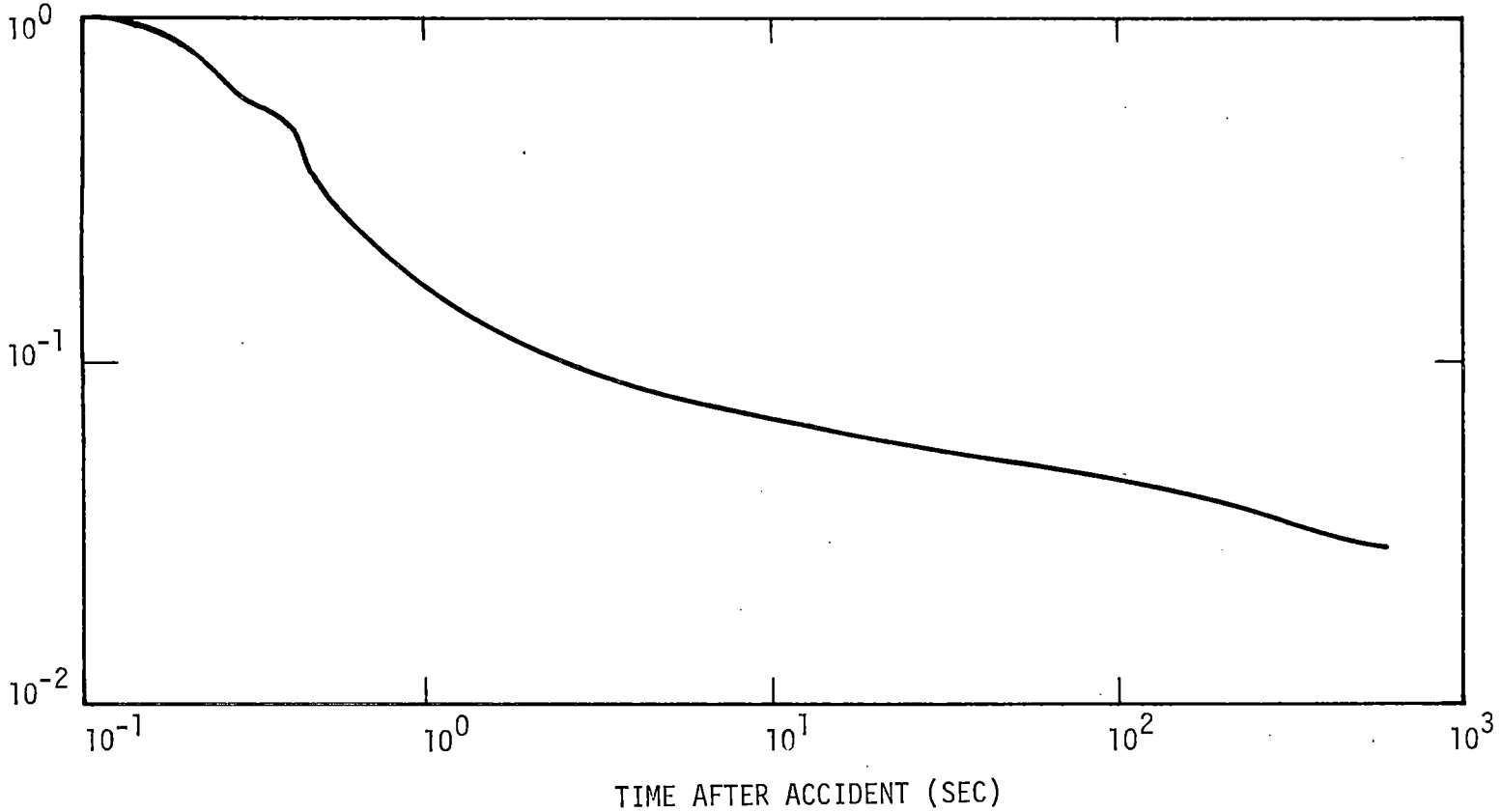

FIGURE III-3 - NORMALIZED POWER FOLLOWING RECIRCULATION LINE BREAK

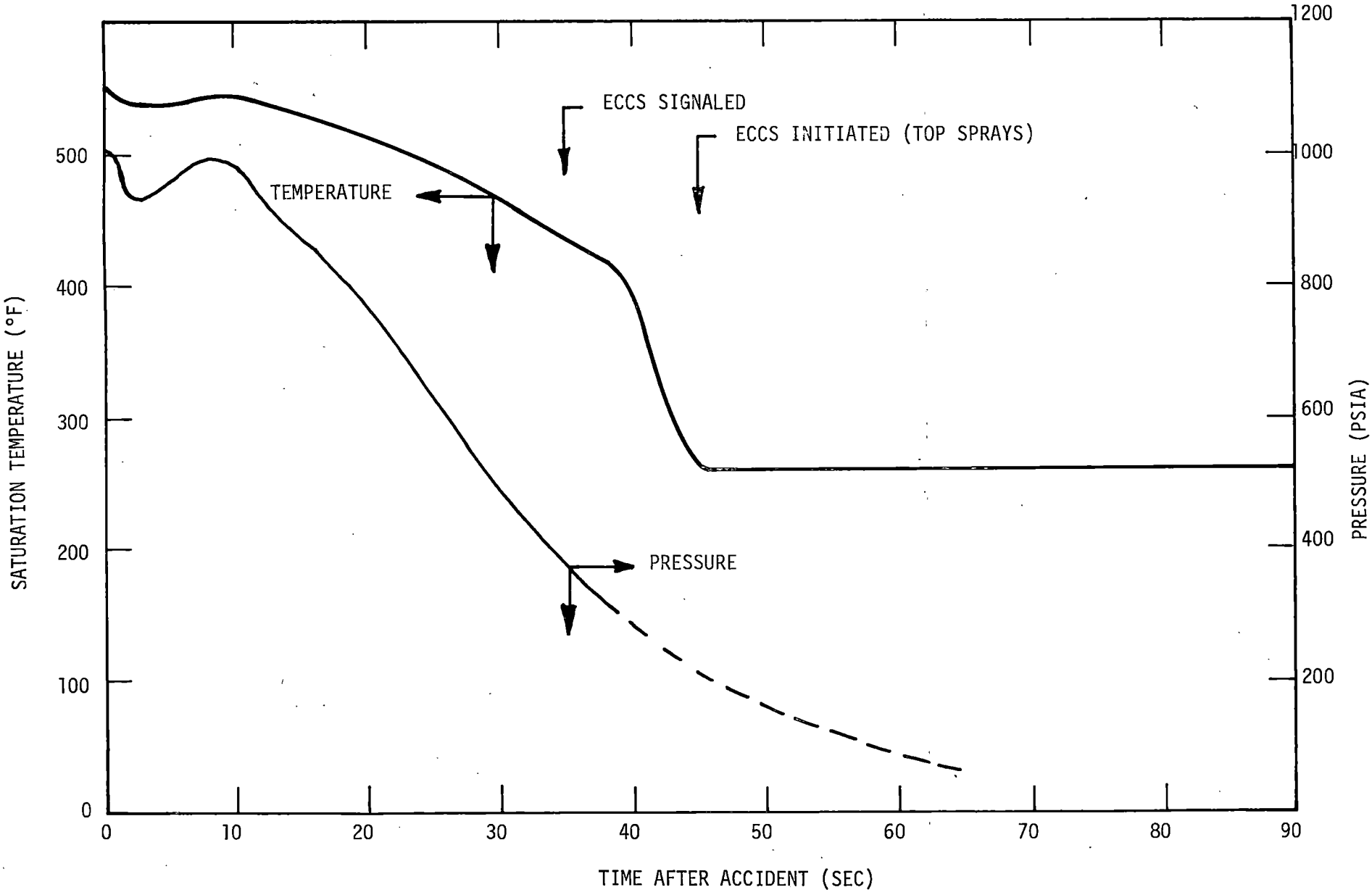

FIGURE III-4 - SATURATION TEMPERATURE AND PRESSURE FOLLOWING RECIRCULATION LINE BREAK

for top spray was taken and no core heat transfer was assumed for the MOXEI calculations during this 10 second period of time.

The calculated heat transfer coefficients for both the hot channel and average channel during blowdown are shown in Figure III-5. These coefficients were utilized in the core heat-up calculation which is discussed in detail in the following sections.

The worst case assumption of two core spray systems only was utilized in conjunction with the top spray only heat transfer coefficients specified in 10 CFR 50.46. The RELAP4 blowdown results were used to determine the liquid volume inventory in the lower plenum at the time the core sprays were assumed operational, i.e., 45 seconds. The spray water was assumed to penetrate the core and evaporate at a rate of 1.8 ft^3/second. This evaporation rate corresponds to the latent heat of vaporization equivalent to removal of 4 percent of core power. The liquid accumulation in the lower plenum from the remainder of the core spray resulted in the liquid level reaching the bottom of the active core region at 212 seconds after blowdown initiation. The equivalent cold flooding rate in the core was 1.5 inches per second. The water level reached the hot spot in an additional 38 seconds assuming no bubble rise or level swell effects. The levels considered were for liquid water with no entrained vapor bubbles. When the liquid level reached the hot spot a constant heat transfer coefficient of 25 BTU/hr-ft^2-°F was utilized as shown in Figure III-6.

1.1.2.2 MOXEI Results

As stated above, the heat transfer coefficients determined by the RELAP4 calculation were utilized for the blowdown phase of the core heat-up calculation and the constant values, as specified in 10 CFR 50.46, for the ECC injection phase is shown in Figure III-6. The core hot spot blowdown heat transfer coefficients as calculated by RELAP4 were used for all the axial regions considered during the blowdown phase of the core heat-up calculations.

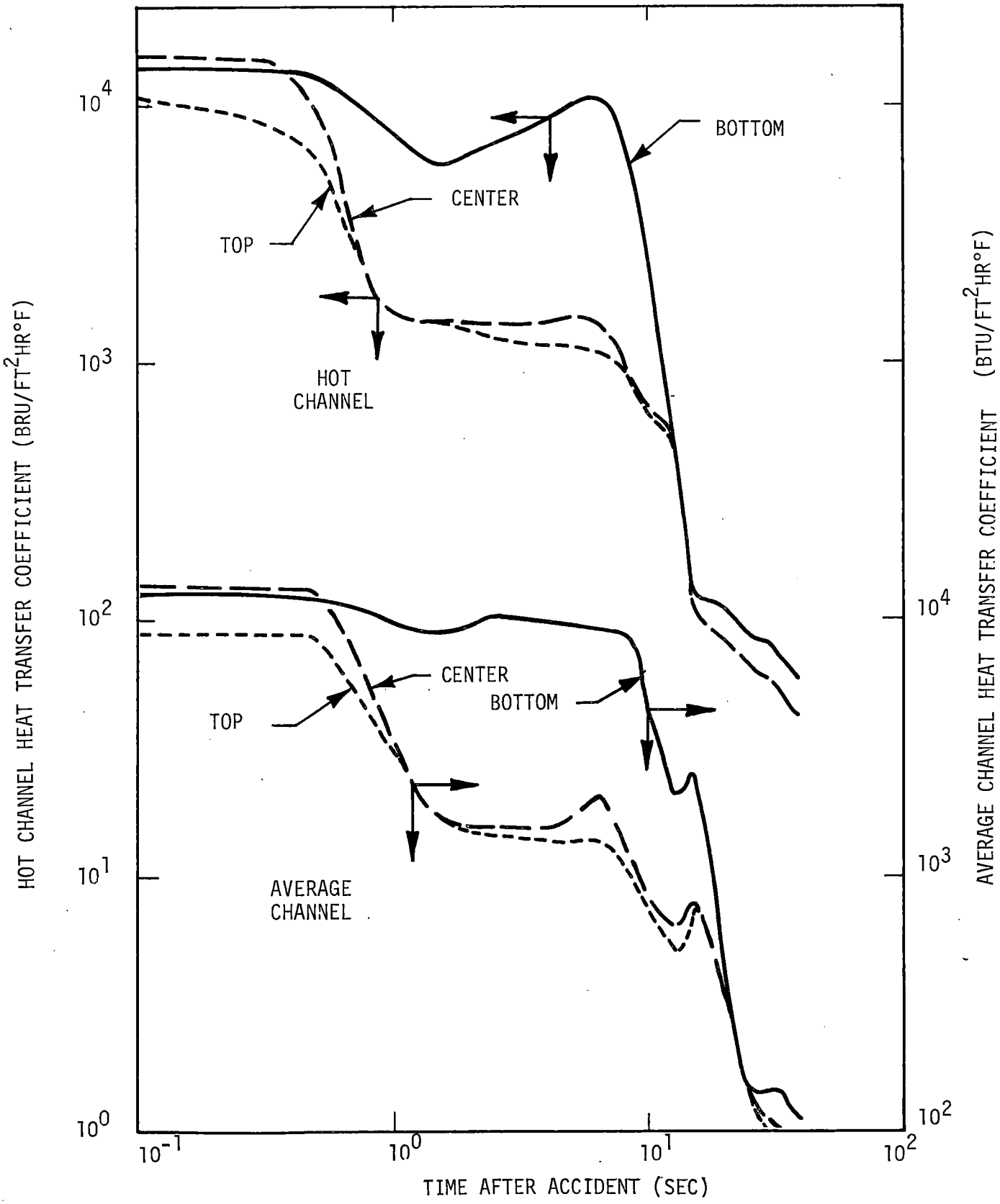

FIGURE III-5 - HEAT TRANSFER COEFFICIENTS DURING BLOWDOWN FOR THE HOT CHANNEL AND AVERAGE CHANNEL

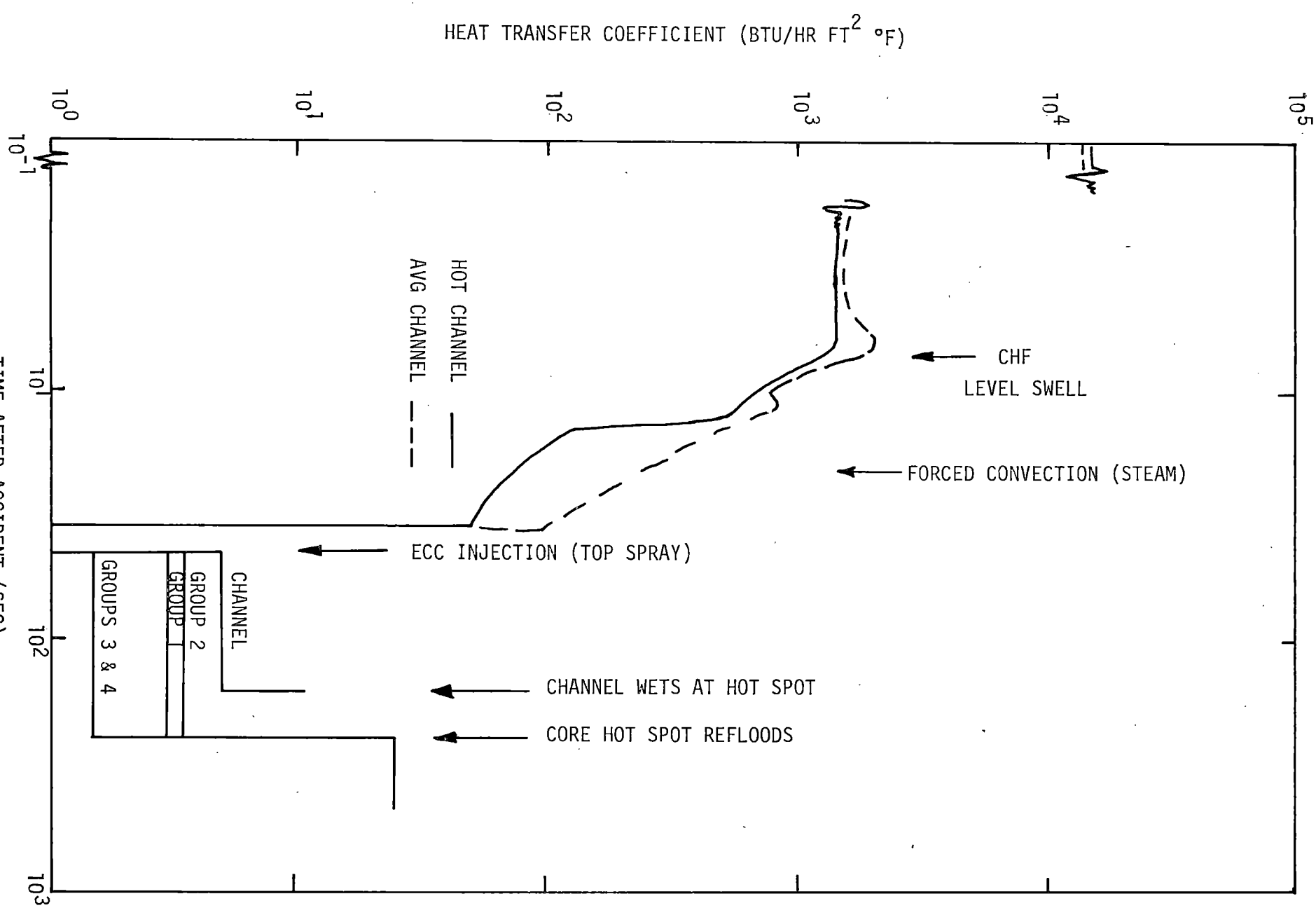

FIGURE III-6 - HEAT TRANSFER COEFFICIENT UTILIZED IN CORE HEAT-UP CALCULATIONS FOR THE HOT AND AVERAGE CHANNELS

The core heat-up calculations were performed for a total of ten cases o the twelve possible combinations. The case distribution for combinatio of the core axial and radial peaking factors is shown in Table III-II. Table III-II shows both the total possible combinations and the actual combinations used in this calculation. Combinations of cases and deleti of the ballooning considerations were made when the peak temperatures were less than that required for ballooning. The calculated temperature responses for a rod in each of the four rod groups at the core hot spot are shown in Figures III-7 and III-8. These temperatures for the core hot spot are the calculational results for both the ballooned and non-ballooned rod sections. The difference in peak temperature was approximately 200 F° between the ballooned and the non-ballooned rod segments. The peak temperature of 2185°F occurred at the time of flood on the ballooned rod surface. For this calculation the channel wetting time was computed to be 160 seconds after accident initiation for the channel hot spot. The channel wetting time calculation included the 60 second margin and time to spray initiation added to the calculated time from the Yamanouchi correlation as required by the criteria. The wetting times for the remaining cases were calculated in the same manner taking into account the elevation and temperature differences.

The hydrogen generated during the core heat-up calculations was tabulated for each case of the segmented core and these tabulations are shown in Table III-III as cumulative weighted fractions. The values of hydrogen fractions in percent are weighted against the total core. Thus, the values are percent theoretical zirc reacted in each segment multiplied by the volume fraction of total zirc in the core for which the particular segment represents. The cumulative total shown in Table III-III is obtained by summing the weighted fraction of each segment.

As can be seen from the total accumulation, less than 0.1 percent of the zirc in the core has reacted. Two functional graphs of the hydrogen generation are presented in Figures III-9 and III-10. The first illustrates the hydrogen generation rate as a function of time. The second presents the total cumulative generation. These figures are graphical representations

TABLE III-II

SPECIFICATION OF THEORETICAL AND ACTUAL CORE HEAT-UP CALCULATION CASES

Possible Case ID Number	Axial Peaking Factor (1)	Radial Peaking Factor (2)	% Core Volume Represented	Actual Case ID
1	1.57	1.47	3.583	1
1B*	1.57	1.47	0.417	1B
2	1.57	1.10	8.958	2
2B*	1.57	1.10	1.042	2
3	1.57	0.8	5.375	3
3B*	1.57	0.8	0.625	3
4	1.3	1.47	6.0	4
5	1.3	1.10	15.0	5
6	1.3	0.8	9.0	6
7	0.7	1.47	10.0	7
8	0.7	1.10	25.0	8
9	0.7	0.8	15.0	9

* B refers to ballooned case consideration.

(1) See axial profile in Figure A-2

(2) See radial profile in Figure A-6

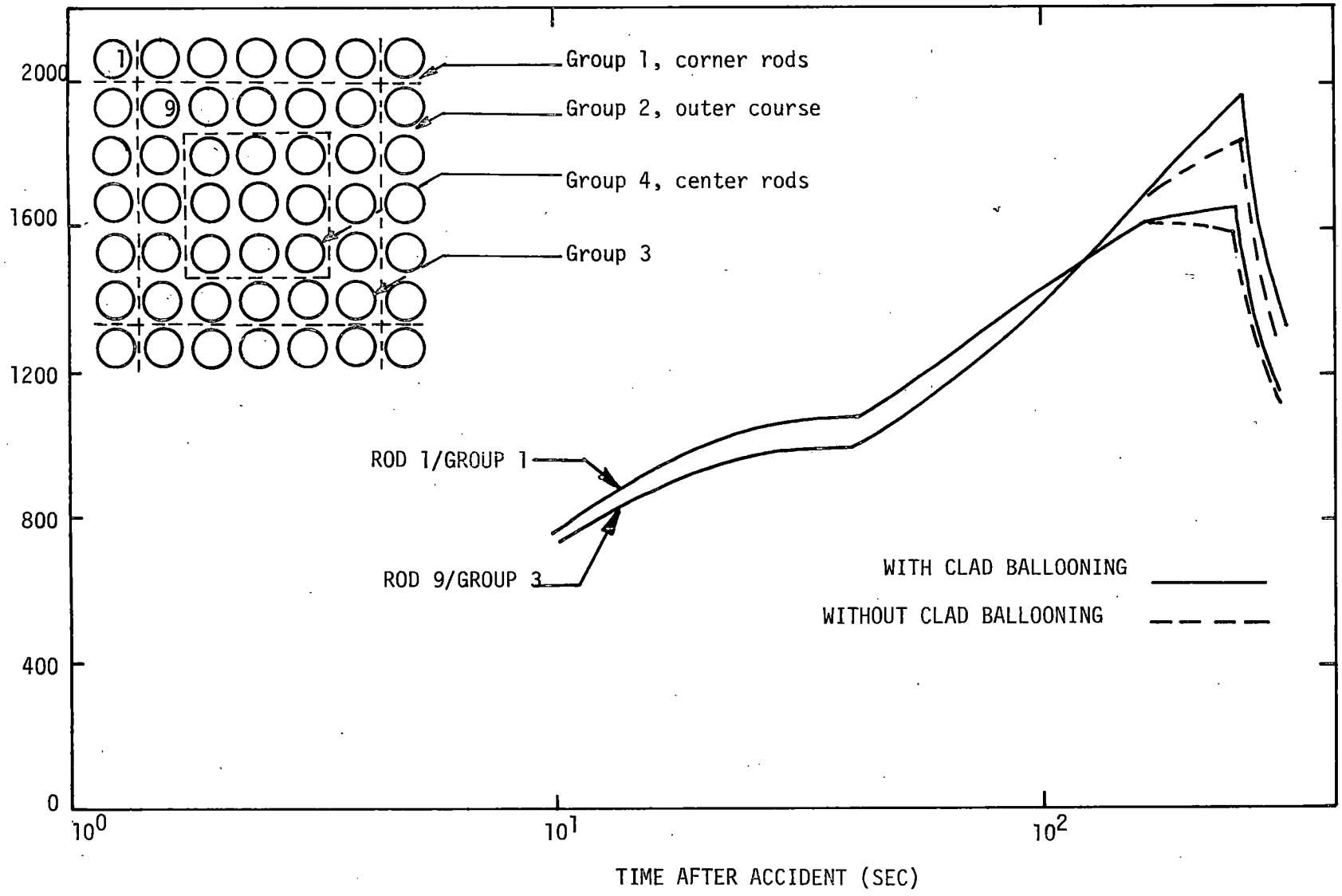

FIGURE III-7 - TEMPERATURE RESPONSES FOR RODS IN GROUPS 1 AND 3 AT THE CORE HOT SPOT

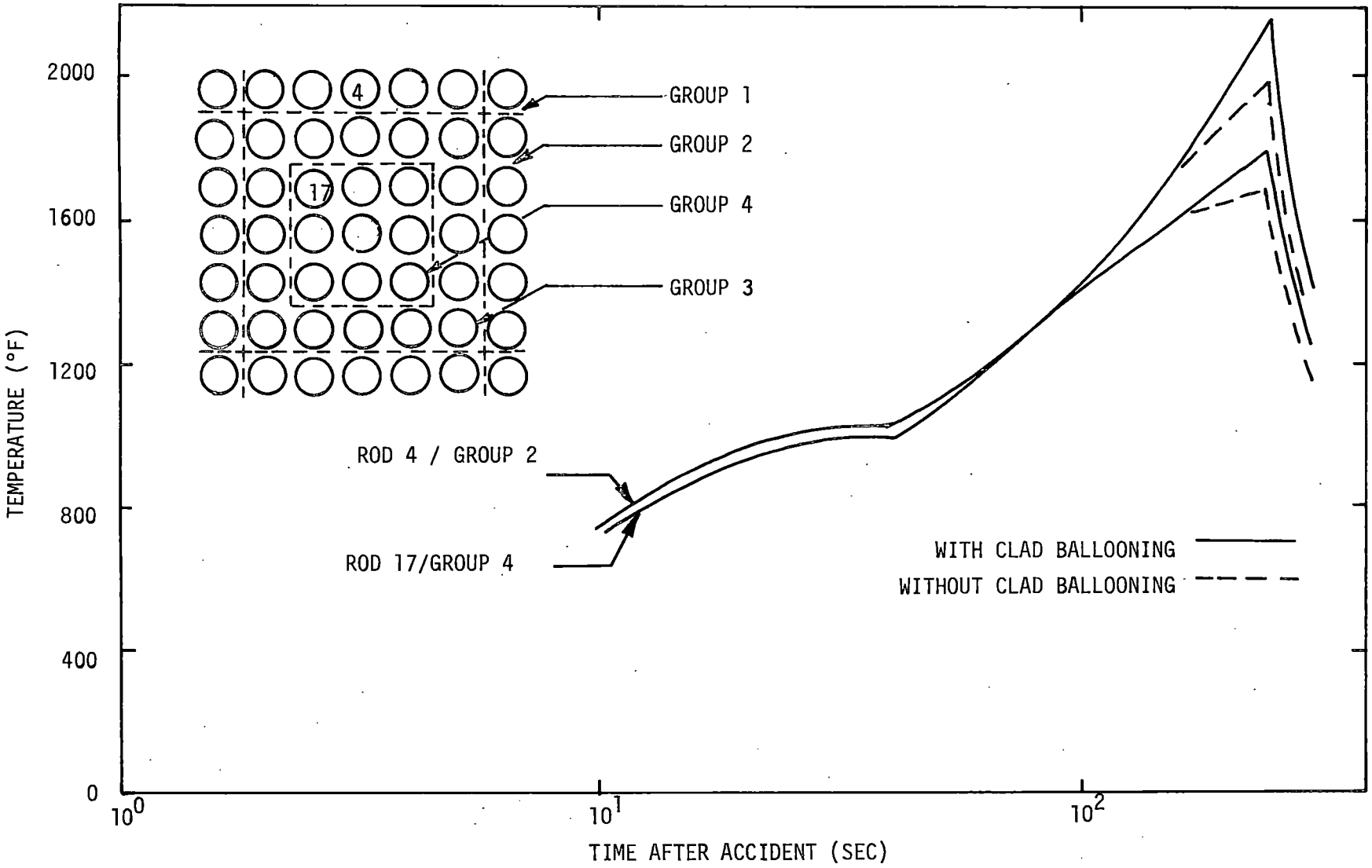

FIGURE III-8 - TEMPERATURE RESPONSES FOR RODS IN GROUPS 2 AND 4 AT THE CORE HOT SPOT

TABLE III-III

WEIGHTED PERCENT FRACTIONS OF ZIRC REACTED FOR EACH CORE SEGMENT

Time	Case ID (Table 2)								Total
	1	1B	2	3	4	5	6	7	
40									
60	.0000731	.0000085							.0000815
80	.000438	.000051			.000245				.000734
100	.00139	.000162			.000734				.002286
120	.00314	.000366	.000408		.00171				.00562
140	.00585	.000757	.00102		.00355	.000306			.01148
160	.00957	.00195	.00204	.000122	.006	.000612		.0002	.02049
180	.01396	.00381	.00367	.000122	.0093	.00153		.0002	.032592
200	.0188	.00586	.00591	.000367	.0132	.00275	.00018	.000408	.04747
220	.024	.00855	.00836	.000612	.0174	.00398		.000612	.06351
240	.0297	.0117	.01142	.000857	.0216	.00581	.00037	.000816	.08227
260	.0335	.0142	.01346	.0011	.0246	.00704	.00037	.00102	.09529
280	.0337	.0144	.01366	.0011	.0247	.00704	.00037	.00102	.09599
300	.0338	.0144	.01366	.0011	.0247	.00704	.00037	.00102	.09609

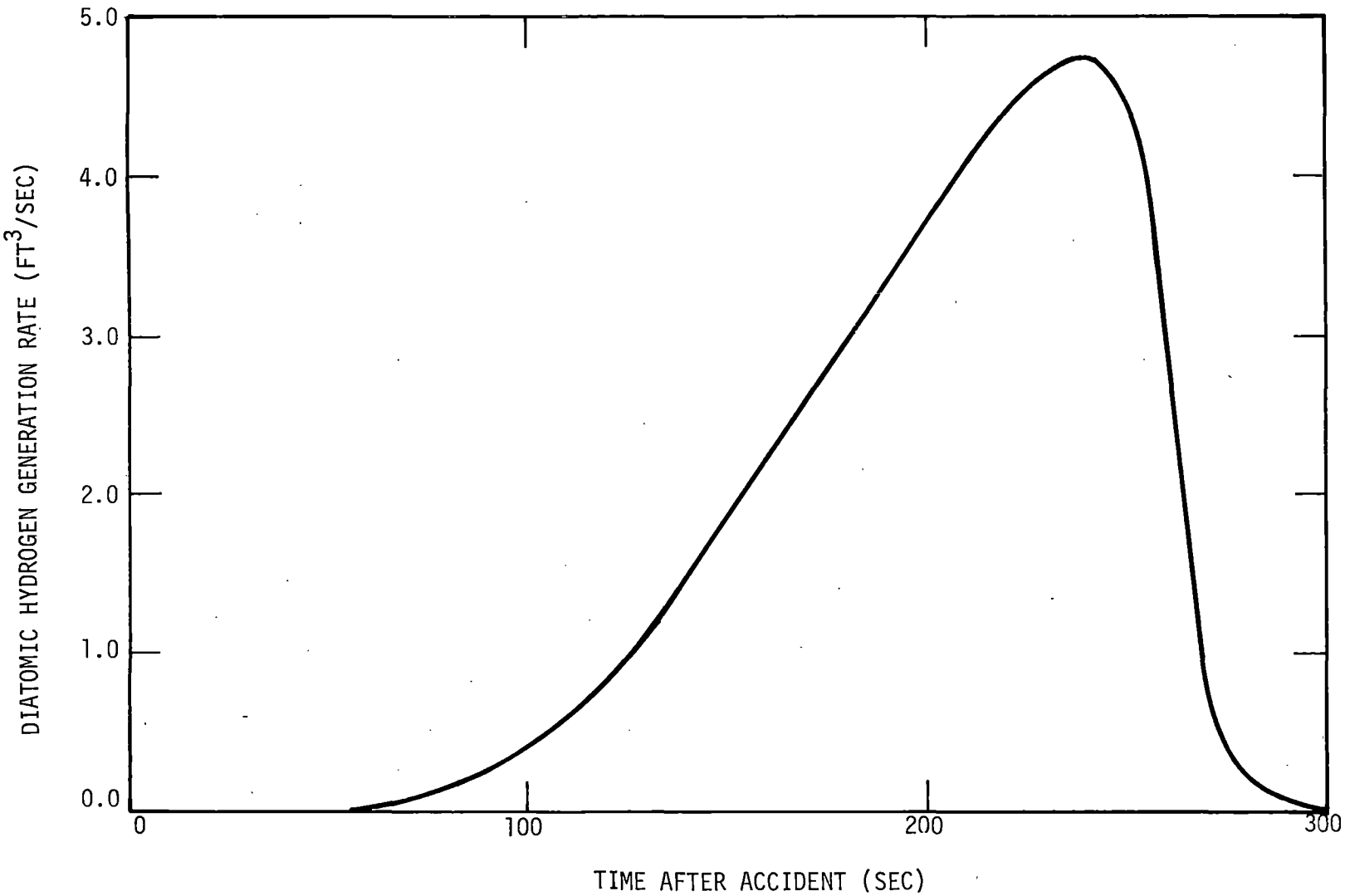

FIGURE III-9 - HYDROGEN PRODUCTION RATE FOLLOWING BREAK IN RECIRCULATION LINE

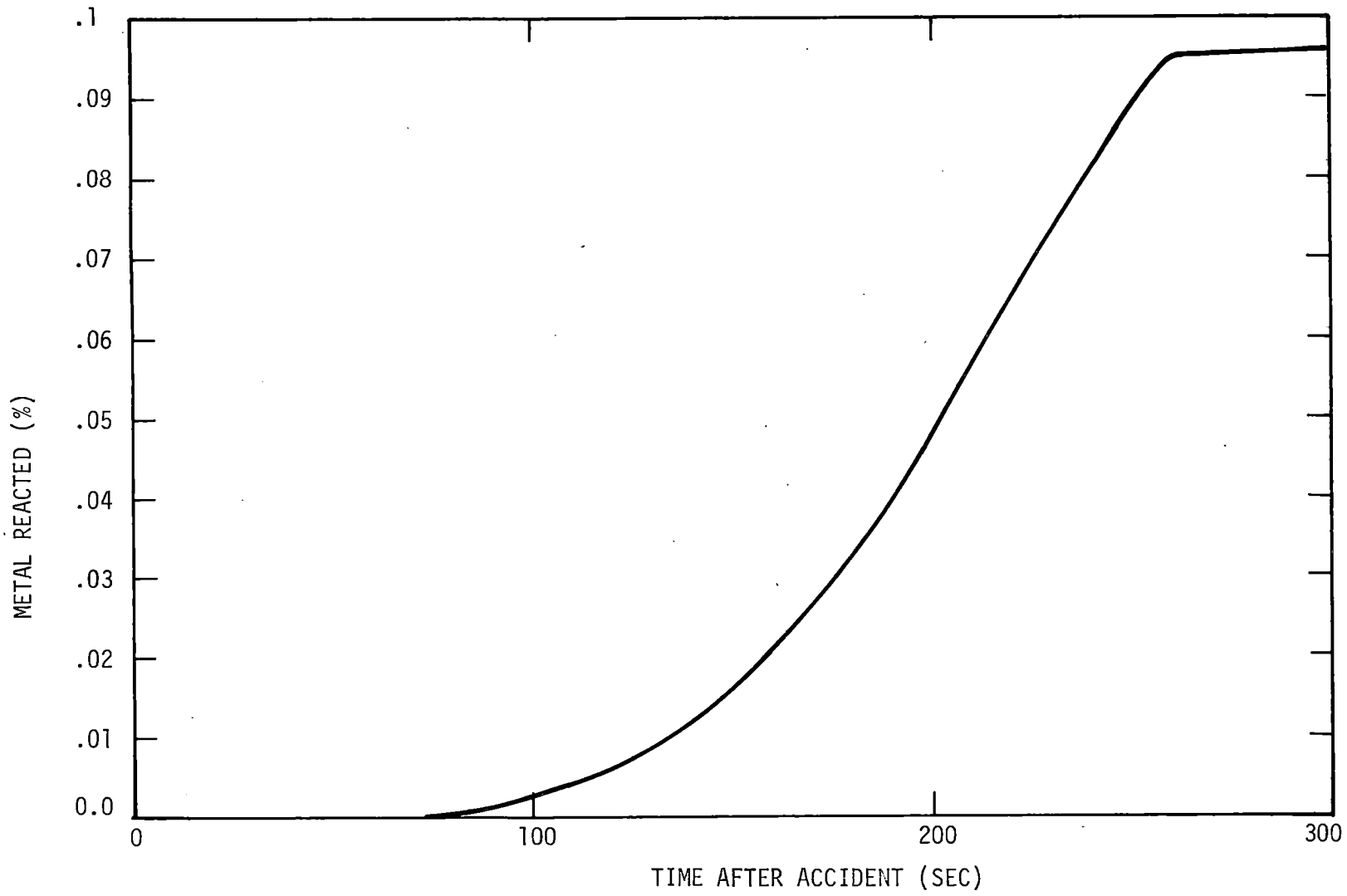

FIGURE III-10 - CUMULATIVE METAL-WATER REACTION (% Zr REACTED/INITIAL Zr METAL)

of the data shown in Table III-III. Note that no hydrogen generation was calculated for Cases 8 and 9 of Table III-III. Peak temperatures for these two cases were too low for noticeable metal-water reaction. On a volume basis, Cases 8 and 9 represent a total of 40 percent of the volume of zirc in the core.

1.1.3 Minimum Metal-Water Reaction Allowed

The metal-water reaction-generated hydrogen based on a core-wide penetration of 0.00023 inches for 35,476 fuel rods with a cladding thickness of 0.032 inches, arranged in 7 X 7 assemblies, results in a 0.72 percent metal-water reaction or a hydrogen generation rate of 1832.52 SCFM. Utilizing the same cladding penetration for an 8 X 8 assembly results in a core-wide metal-water reaction of 0.68%. Thus, utilizing 0.72% metal-water reaction in the analysis adequately accounts for some 8 X 8 assemblies intermixed with the 7 X 7 assemblies at the plants in question. Since this value (0.72%) for metal-water reaction is greater than five times the maximum calculated (0.5%) metal-water reaction, using the criteria set forth in 10 CFR 50.46, the containment hydrogen concentration and the radiological impact of ACADS is based on this larger value (0.72%) of metal-water reaction.

1.2 Radiolytic Hydrogen and Oxygen

Generation of radiolytic hydrogen and oxygen becomes an important factor in the long term hydrogen buildup calculations. The approach used in this analysis was to comply with the assumptions outlined in the August 14, 1974 draft of Regulatory Guide 1.7, i.e., it was assumed that 0 percent of β radiation and 10 percent of γ radiation from fission products in the fuel is absorbed in the coolant contained in the core region and 100 percent of β and γ radiation from fission products intermixed with coolant are absorbed in the coolant. Figure III-11 shows the resulting energy available for radiolysis in the core and the suppression pool. Figures III-12 and III-13 were generated utilizing the G, γ and β absorption values given in Regulatory Guide 1.7 for hydrogen and oxygen.

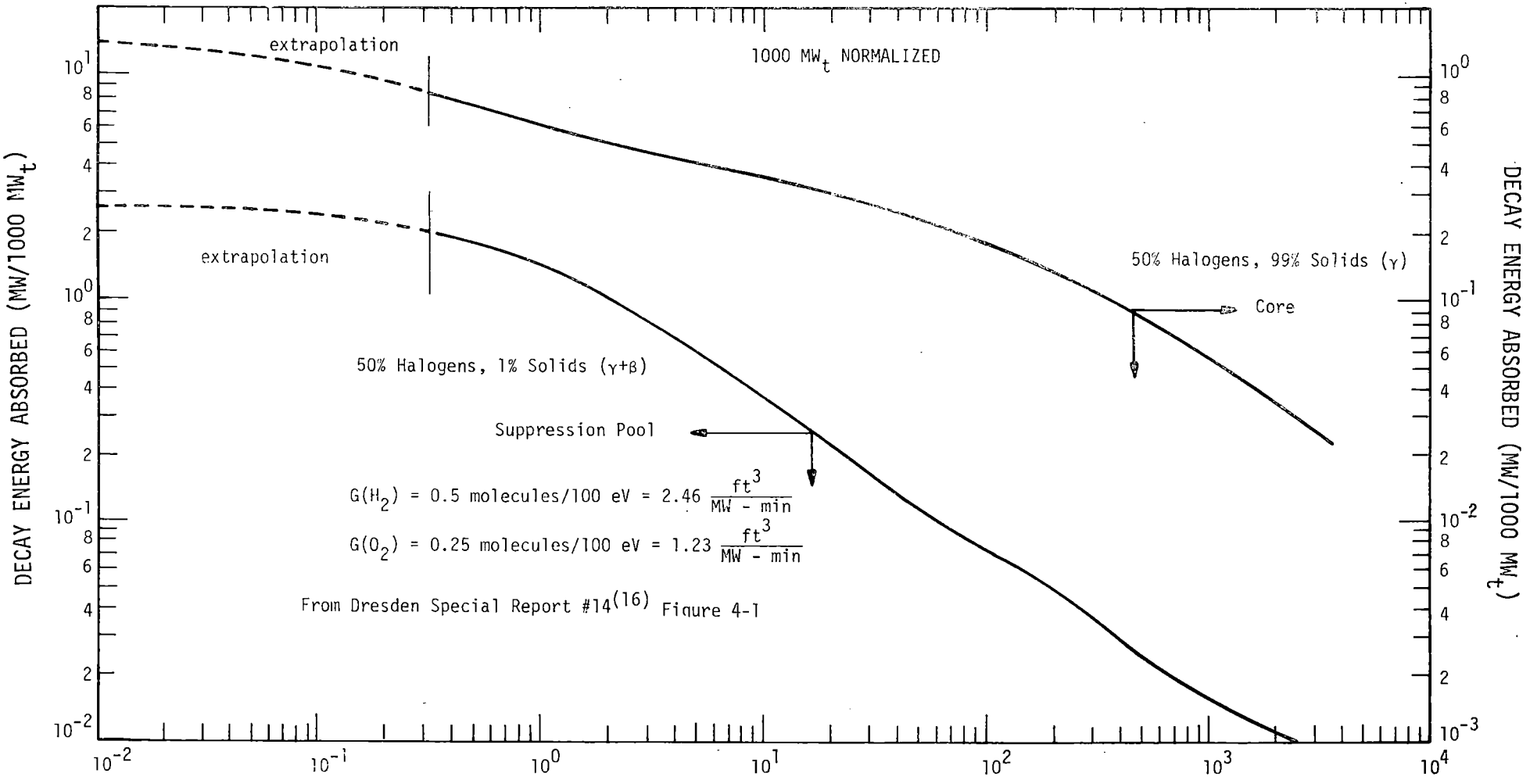

FIGURE III-11 - ENERGY AVAILABLE FOR RADIOLYSIS

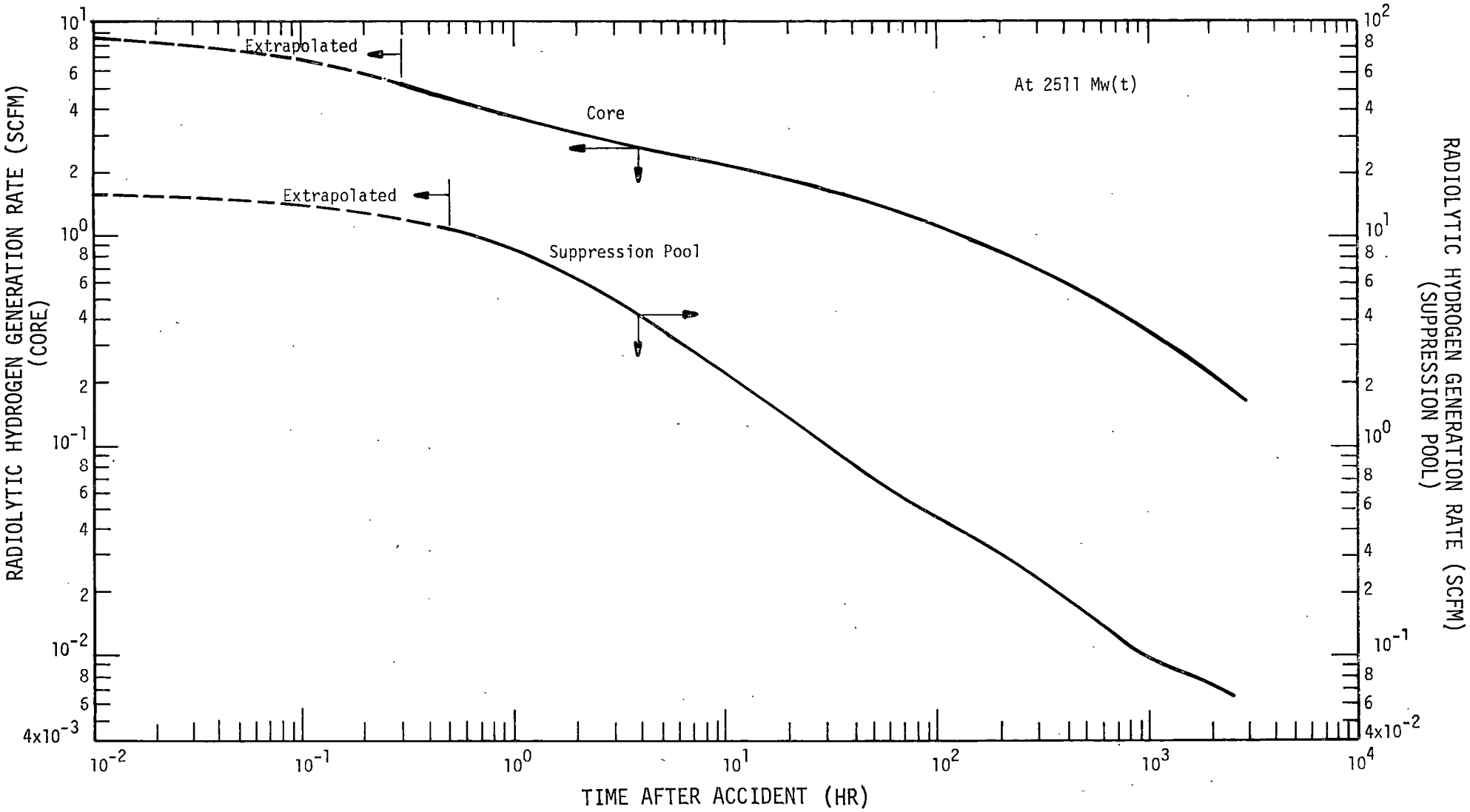

FIGURE III-12 - HYDROGEN GENERATION RATE

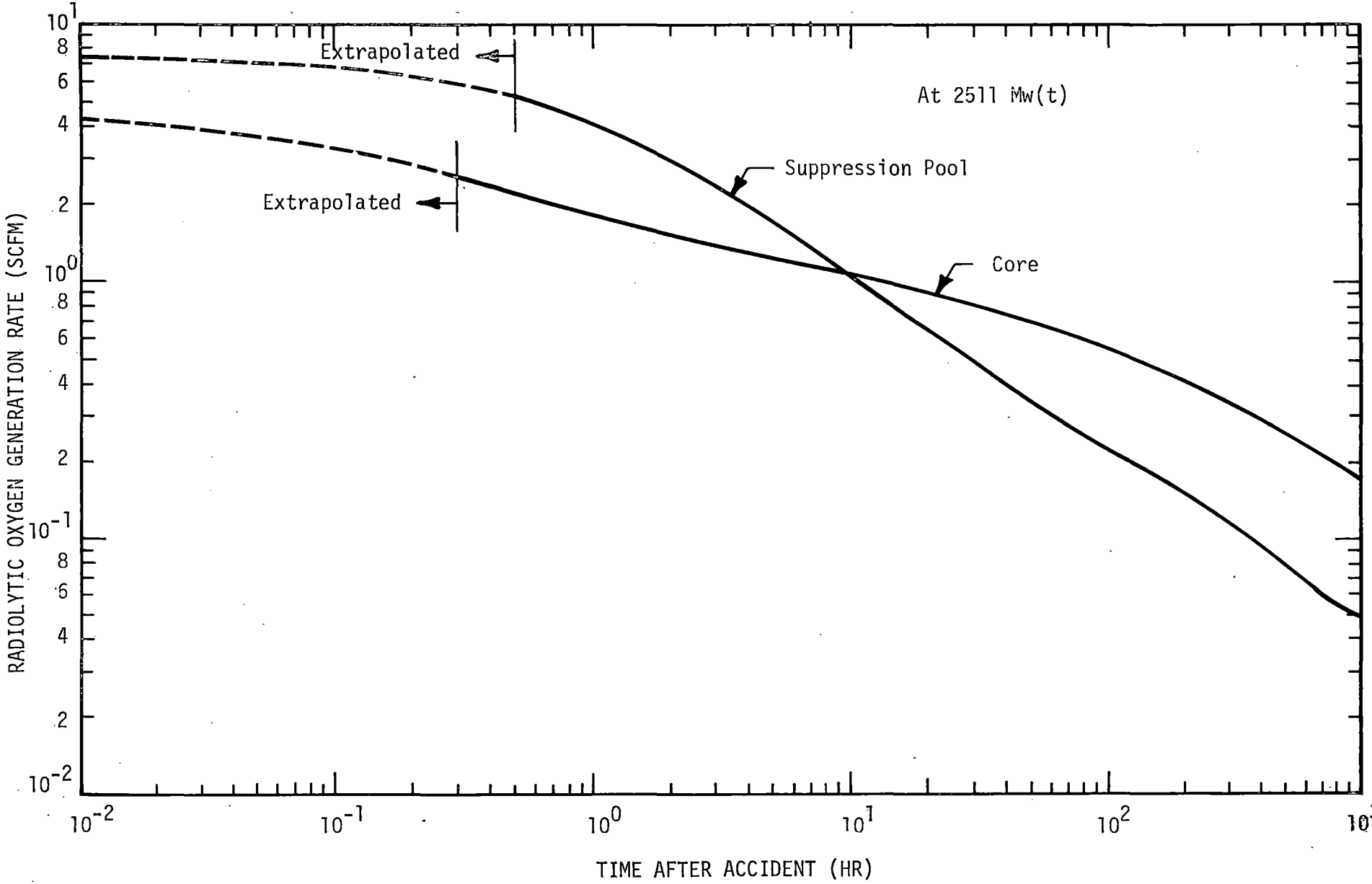

FIGURE III-13 - OXYGEN GENERATION RATE

1.3 Other Sources of Hydrogen

There is a possibility in light-water reactors for hydrogen to be generated after a LOCA from several other sources such as corrosion and reaction of materials inside the drywell and suppression pool with the post-LOCA environment. Of all the sources considered, the reaction with zinc in paint coatings and reaction with galvanized ductwork were thought to be of significance.

Further investigation of Figures III-14, III-15, and III-16 as well as referring to References 19, 20 and 21 show that the contribution from these two sources would be minimal if not negligible. It can be seen from Figure III-14 and III-15 that the temperature in the drywell reaches and exceeds a temperature of 107°C (225°F) for no more than 12 minutes. The rest of the time the temperatures are below 107°C (225°F). Figure III-16 shows that temperatures in the suppression pool never reach 107°C. The tests described in the above mentioned reports were conducted at temperatures of 107°C for 22 hours and 15 minutes, 140°C for 1 hour and 45 minutes and 149°C for 5 minutes and for that cumulative period of time hydrogen yields did not exceed 2.5 cm^3/cm^2. A hydrogen yield of 2.5 cm^3/cm^2 corresponds to approximately 1 v/o hydrogen within the containment. By comparing the conditions in the drywell to those in the tests, it was concluded that the hydrogen yields obtained in the tests are by far greater than those which wuld be obtained following LOCA in a Mark I containment. Consequently, the contributions from these sources are negligible.

Prior to a LOCA, there are system leaks within the drywell and the hydrogen produced as a result of these leaks has been taken into account. It was arbitrarily assumed that a leak identical to the technical specifications limit of 5 gpm existed for three months prior to the postulated LOCA. A leak of this size will introduce 2 lb moles of hydrogen into the containment atmosphere. However, there will be approximately 50 ventings of the containment during a three month period and the resulting concentration was calculated to be approximately one-third of the original value.

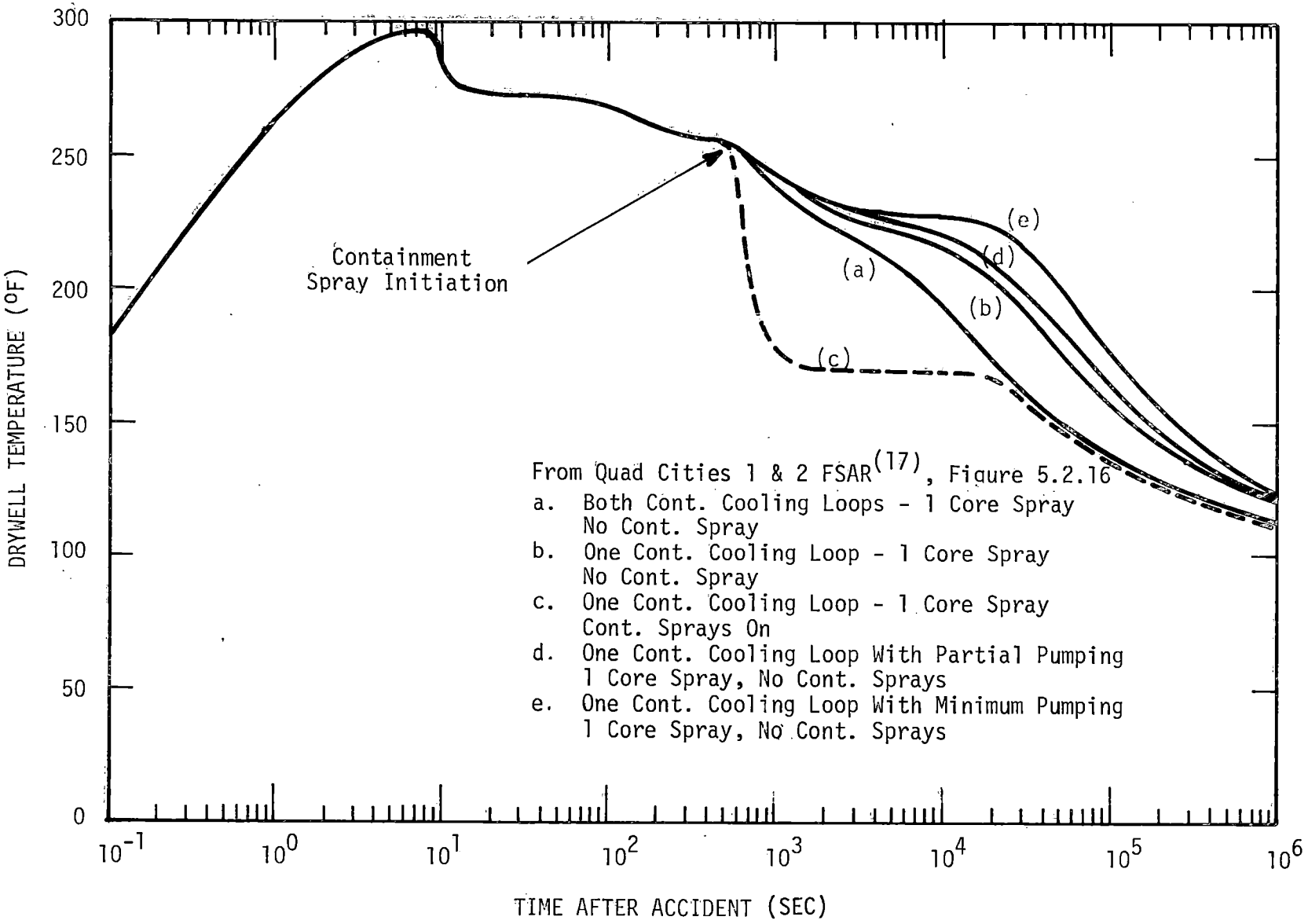

FIGURE III-14 - DRYWELL TEMPERATURE RESPONSE FOLLOWING DESIGN BASIS LOSS-OF-COOLANT ACCIDENT

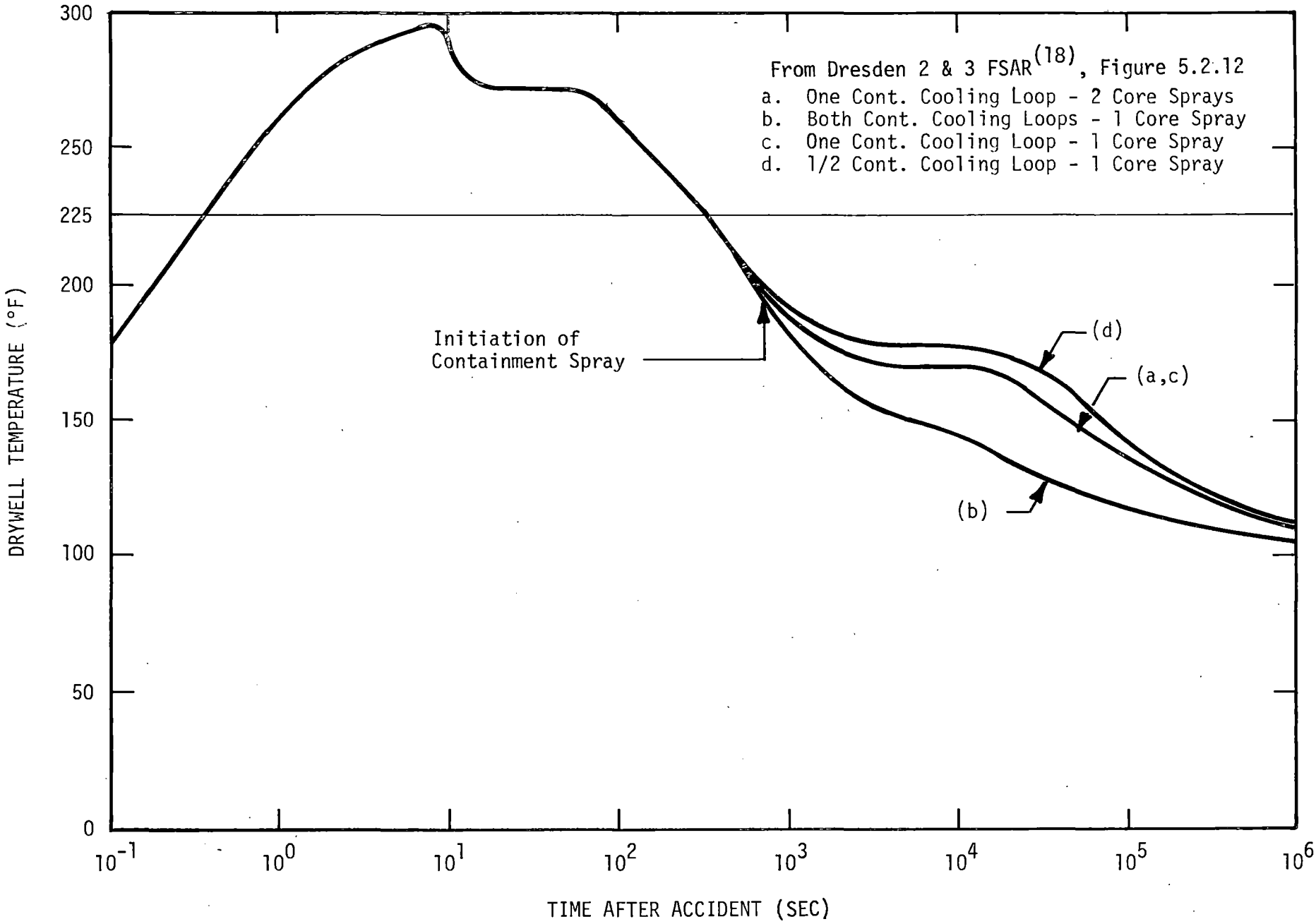

FIGURE III-15 - TEMPERATURE RESPONSE TO LOSS-OF-COOLANT ACCIDENT

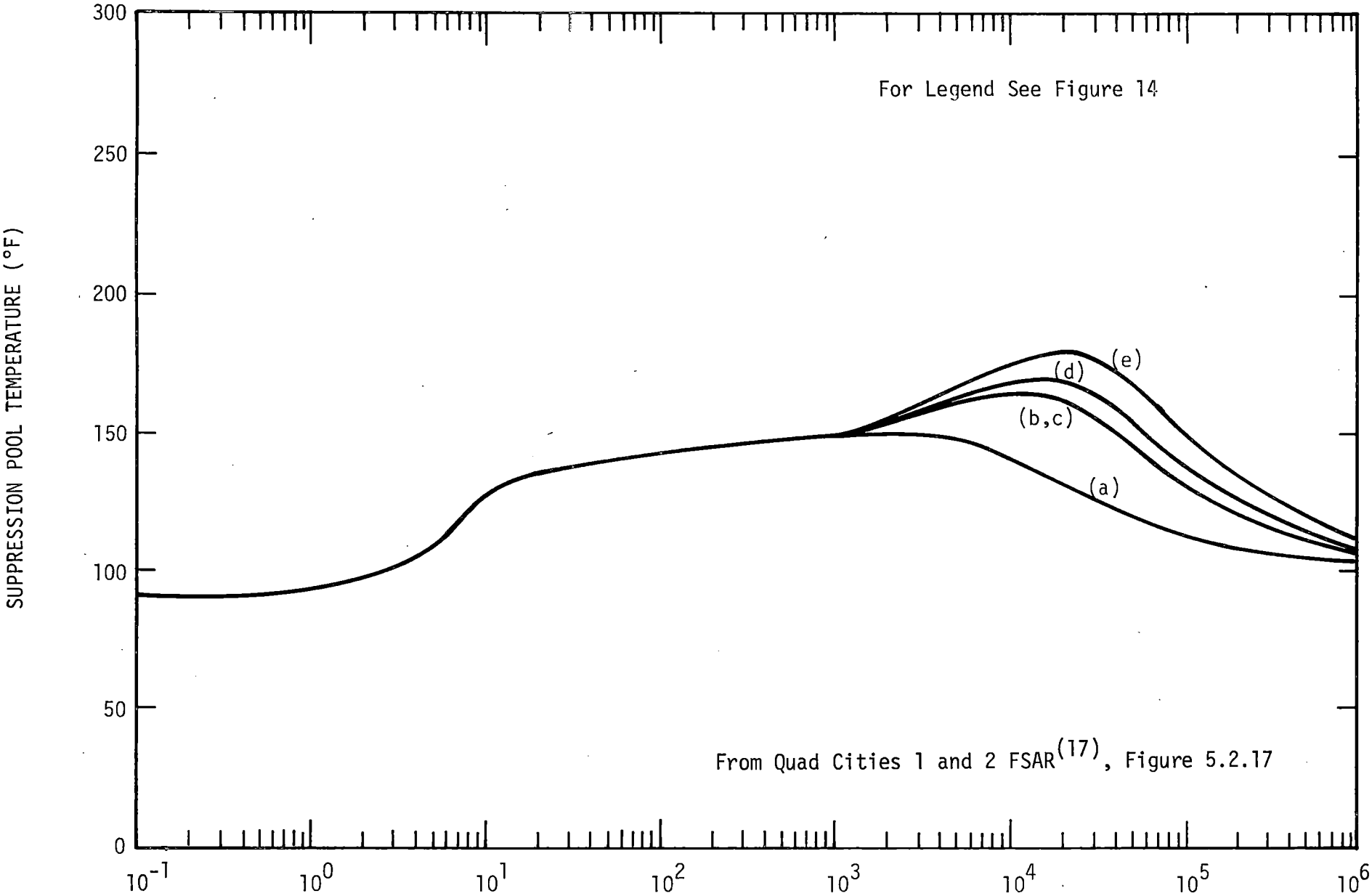

FIGURE III-16 - SUPPRESSION POOL TEMPERATURE RESPONSE FOLLOWING DESIGN BASIS LOSS-OF-COOLANT ACCIDENT

2.0 CALCULATION OF CONTAINMENT HYDROGEN CONCENTRATION

2.1 Containment Model

In formulating the model of the Mark I containment for these calculations, two coservative assumptions were made. First, the suppression pool and the drywell were treated as two totally isolated and independent volumes. Thus, no credit has been taken for the effect of blowdown of the drywell volume into the suppression pool, or for the dilution effect of vacuum breakers opening. Secondly, the effect of steam atmosphere, i.e., steam dilution has been neglected.

The model then consists of two separate volumes across which a mass balance of hydrogen and oxygen is computed. The equations describing this mass balance consists of a production term, i.e., hydrogen and oxygen sources, a loss term stemming from the containment leakage (see Figure III-17) and intermittent purges, and a dilution term from the intermittent operation of the atmospheric containment atmosphere dilution system (ACADS). The details of this model are presented in Section A.3 of Appendix A.

2.2 Hydrogen Control Scheme

Throughout this analysis the concentration of hydrogen in the containment was controlled to below 4 v/o since it was assumed that the initial oxygen concentration in the containment was 21 v/o. This was accomplished by initiating the ACADS when the hydrogen concentration in the drywell reached 3.8 v/o. The ACADS flow rate was set to insure that the hydrogen concentration in the volumes would never reach 4 v/o. ACADS was permitted to operate at this rate, pressurizing as well as diluting the drywell and the suppression pool volumes, until the hydrogen concentration in the drywell decreased to below 2.8 v/o. When this concentration was reached, the ACADS was turned off. The pressures in the drywell and suppression pool were monitored by the model during the operation of the ACADS. The pressure in either volume was not allowed to exceed 50 percent of

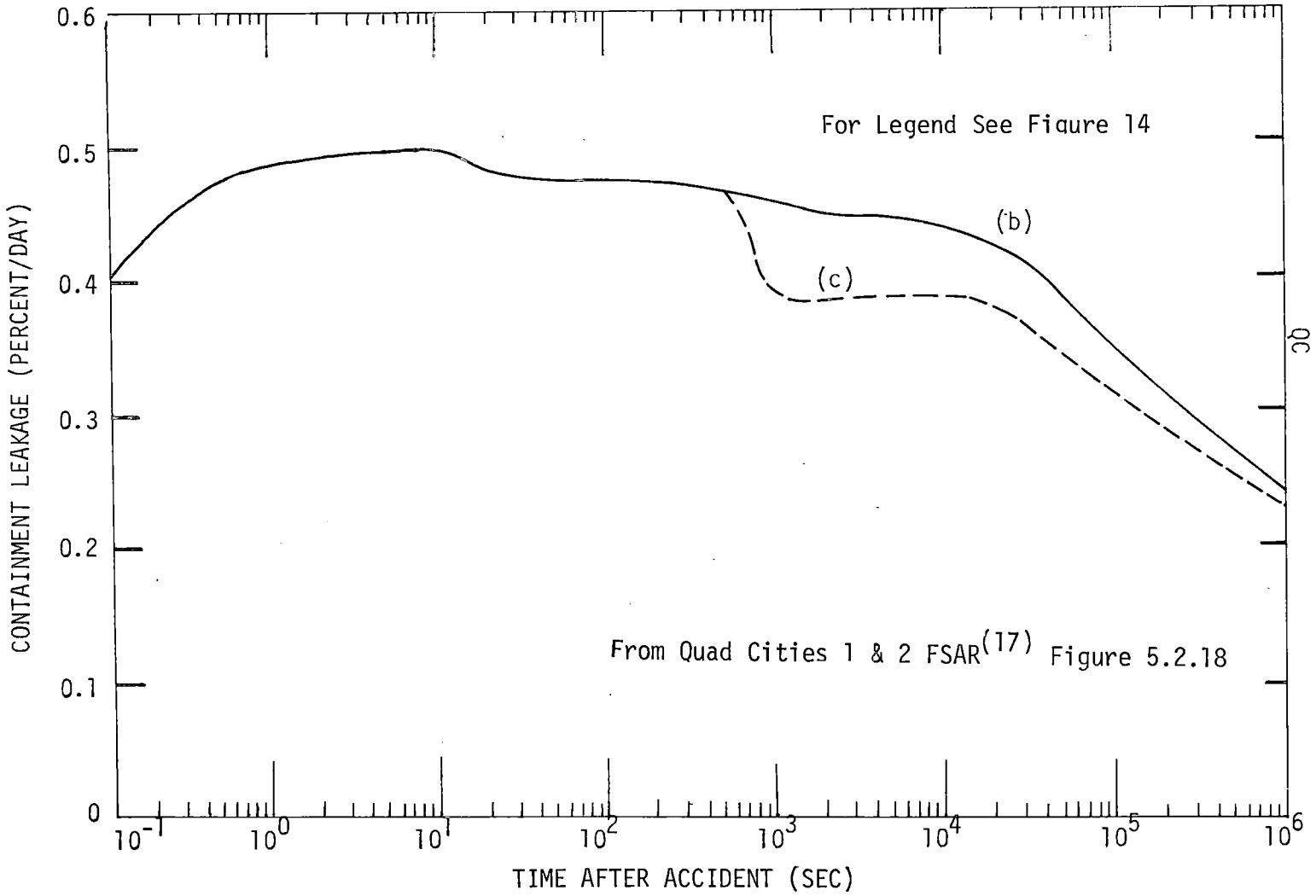

FIGURE III-17 - CONTAINMENT LEAK RATE RESPONSE FOLLOWING DESIGN BASIS LOSS-OF-COOLANT ACCIDENT

their design pressure which in all the plants is 56 psig. When the pressure in either volume reached 50 percent of their design value, the ACADS was shut down and the purging commenced and continued until the pressure dropped to a low set point. This set point was established by taking the minimization of doses as the basic premise and is discussed in the following text.

2.3 Results of Calculations

Calculations of the hydrogen concentration in the containment were performed using the above sources and assumptions as listed in Table III-IV. The results of these calculations are discussed below.

Hydrogen concentration in drywell versus time after LOCA is shown as a solid line in Figures III-18A and III-18B. The hydrogen concentration reached the ACADS cut-on point of 3.8 v/o at 10.92 hours (655 minutes) after the accident. The rate of flow was set at 37.0 SCFM into both the drywell and suppression pool. As is shown by the solid line in Figure III-18B, even though the pressurization commences the hydrogen concentration in the drywell continues climbing up and reaches a maximum of 4.00 v/o at 40 hours (2400 minutes) after the initiation of the LOCA. The concentration then begins to drop slowly. The drywell and the suppression pool are being pressurized as is shown in Figure III-19. Initially the pressures in the two volumes are assumed to be the same. As the time progresses but before the pressurization commences the pressure in the drywell is slightly higher than in the suppression pool. As hydrogen and oxygen are generated in the suppression pool, this pressure difference begins to diminish due to the smaller free volume in the suppression pool. The two pressures are equal again at about 11.5 hours (690 minutes) after the accident and thereafter the pressure in the suppression pool becomes increasingly higher than in the drywell. It must be reiterated at this time that no credit has been taken for the fact that vacuum breakers will fully open and provide dilution for the hydrogen in the drywell when the pressure in the suppression pool is 0.5 psig higher than in the drywell. Neglecting this dilution provides further conservatism to the calculation. When the pressure in the suppression pool reaches 50 percent of

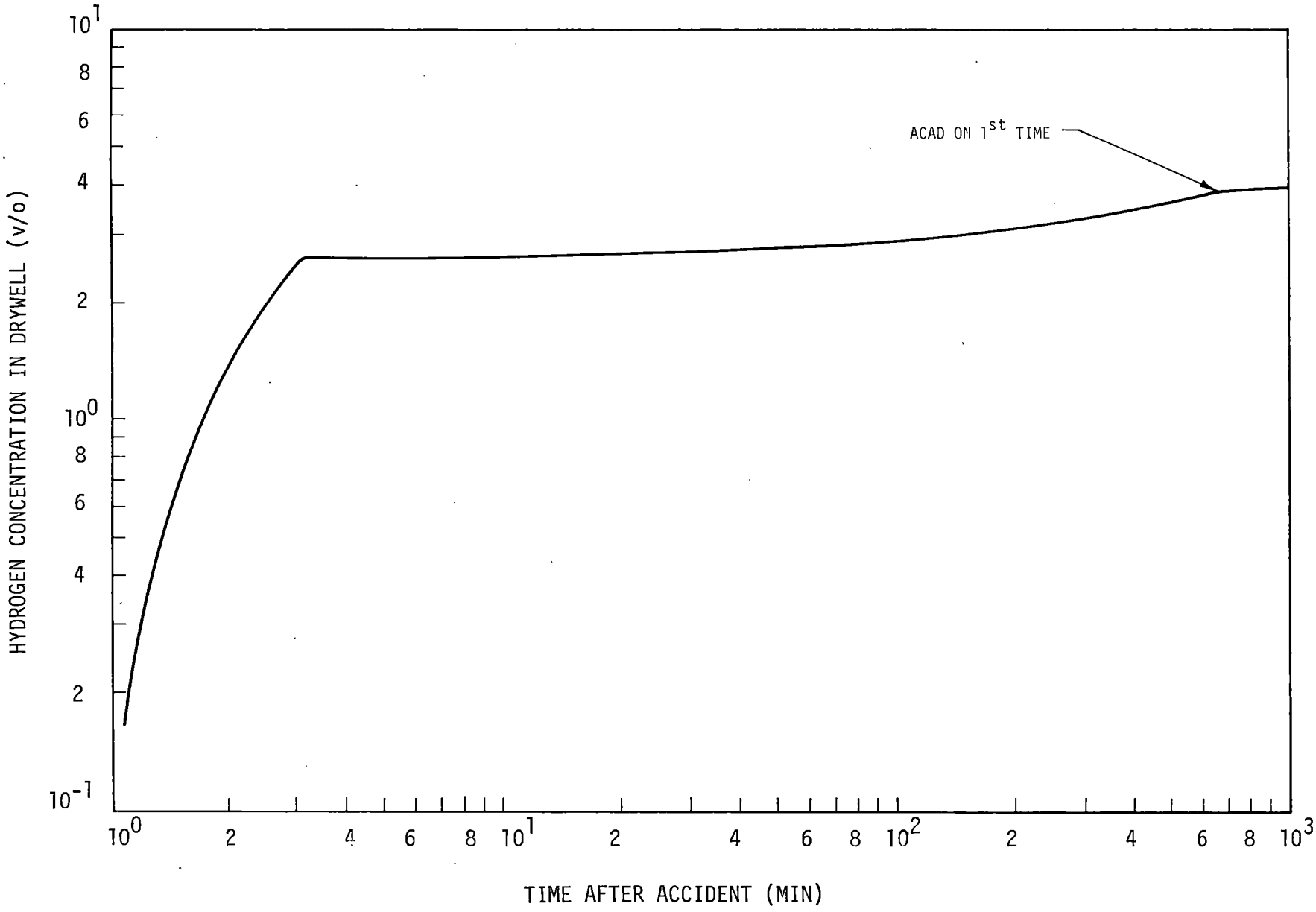

FIGURE III-18A - HYDROGEN CONCENTRATION IN DRYWELL VERSUS TIME AFTER LOCA

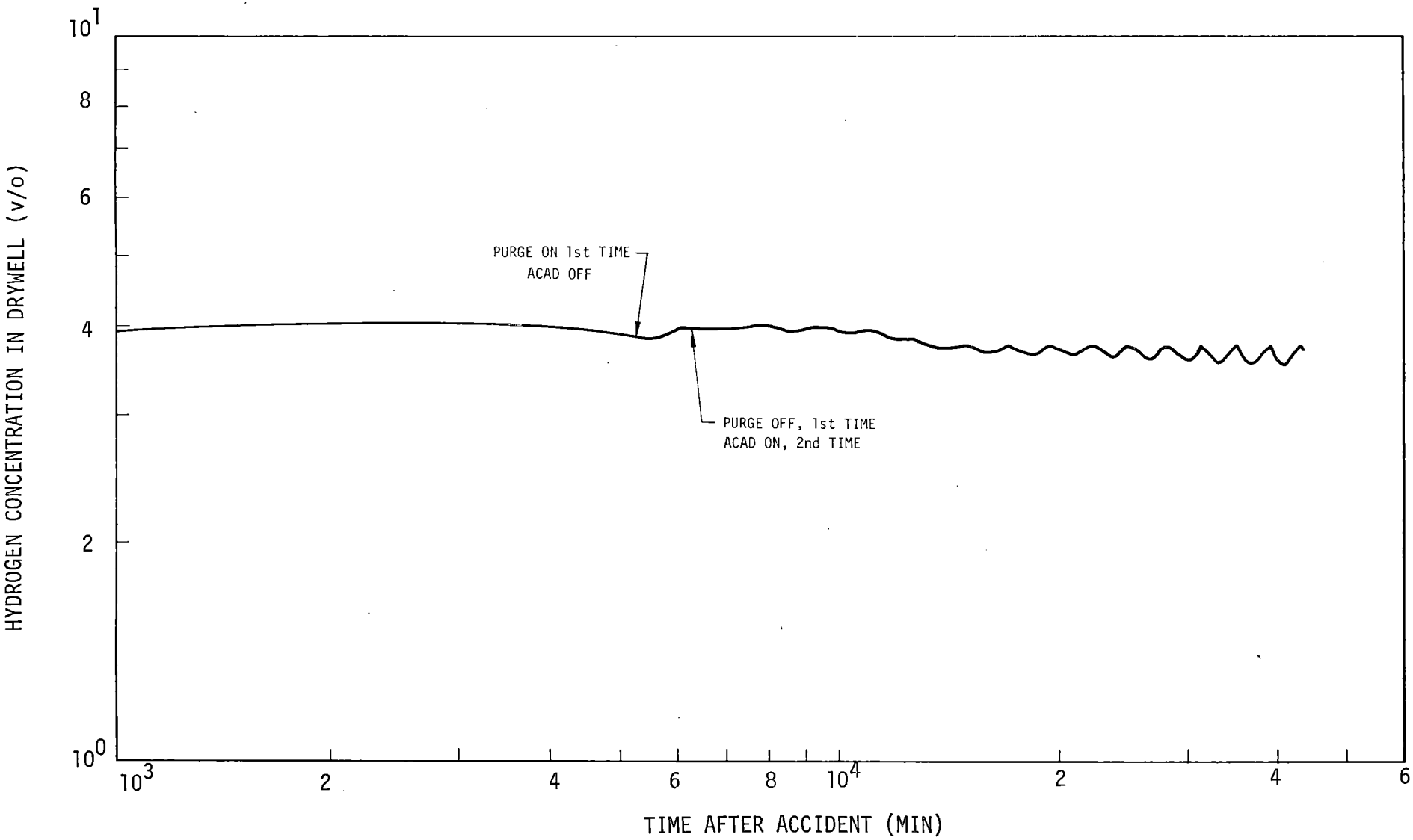

FIGURE III-18B - HYDROGEN CONCENTRATION IN DRYWELL VERSUS TIME AFTER LOCA

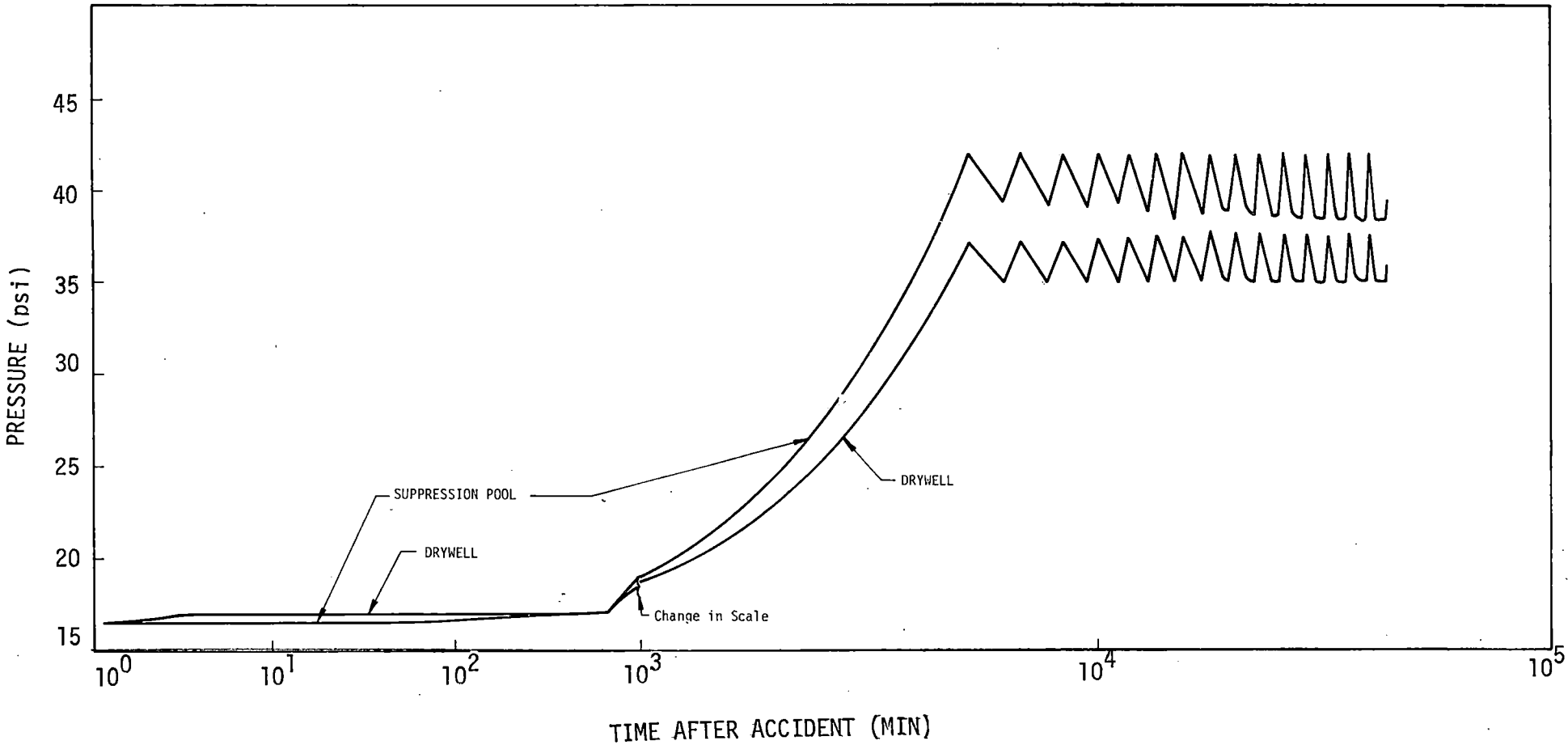

FIGURE III-19 - PRESSURE IN THE DRYWELL AND SUPPRESSION POOL VERSUS TIME

TABLE III-IV

ASSUMPTIONS USED IN CALCULATING HYDROGEN CONCENTRATION VERSUS TIME IN THE CONTAINMENT*

METAL-WATER REACTION	0.72%
GAMMA ABSORPTION PERCENT IN WATER, CORE REGION	10%
$G(H_2)$ IN SUPPRESSION POOL	0.5 molecules/100 ev
$G(H_2)$ IN CORE REGION	0.5 molecules/100 ev
$G(O_2)$ IN SUPPRESSION POOL	0.25 molecules/100 ev
$G(O_2)$ IN CORE REGION	0.25 molecules/100 ev
HYDROGEN CONCENTRATION LIMIT	4 v/o
ACADS PRESSURIZATION FLOW RATE, SCFM	37.0
ACADS PURGE FLOW RATE, SCFM	20.0
CONTAINMENT LEAK RATE	See Figure III-17
INITIAL H_2 CONCENTRATION	1.63×10^{-3} v/o

*All other pertinent assumptions are as specified in the August 14, 1974 draft of Regulatory Guide 1.7.

the design pressure, i.e., 42 psia, the purge is initiated at 20.0 SCFM from both the drywell and the suppression pool. The suppression pool pressure reached 42 psia at 87.42 hours (5245 minutes) or approximately 3.64 days after the accident. In order to minimize the doses, the purge was allowed to continue until the pressure in the drywell dropped to 35 psia. If a higher value for the purge cut-off was chosen, the purge period would be shorter. However, the purge cycling on and off during the duration of the accident would approximate a continuous release. if a lower cut-off or set point is selected, the first purge cycle would last a longer time and prevent holdup of radioactive isotopes inside the containment. As mentioned before, the fact that the vacuum breakers would open and equalize the pressures between the drywell and the suppression pool would, in effect, delay the time at which the purge would first come on.

As it is seen in Figures III-18B and III-19, the pressurization and purging of the two volumes, i.e., drywell and suppression pool continues in cycles with the net result of a release of radioactivity above the radioactivity released during the LOCA.

3.0 RADIOLOGICAL IMPACT OF ATMOSPHERIC CONTAINMENT ATMOSPHERE DILUTION SYSTEM (ACADS)

As is evident from the above discussion, purging of the containment volume is necessary in order to control the hydrogen concentration in the containment to below 4 v/o. Purging of these containment volumes results in incremental doses above the doses calculated for a hypothetical LOCA. Two methods of dose calculations were employed in order to provide a good estimate for these calculations.

The first method, an exceedingly conservative one, provides an estimate of the thyroid dose resulting from the containment purging. This method is the same as the method used by the Staff in their safety evaluation of the Dresden 2 and 3 and the Quad-Cities 1 and 2 units,[22,23] namely, using Regulatory Guide 1.3[24] assumptions. As required by Regulatory Guide 1.7, low population zone 30 day thyroid dose was calculated for the Dresden and Quad-Cities units. Whole body doses were not calculated because it was determined from the staff's safety evaluations for the two plants that the thyroid doses were the controlling doses.

The diffusion factors used for this calculation were those for intermittent releases over the period of 4 to 30 days and evaluated at the low population distance of 3 miles from the Quad-Cities Station and 5 miles from the Dresden Station. The resulting incremental thyroid dose for Quad-Cities and Dresden was 32.8 rem and 21.9 rem, respectively. When added to the highly overestimated LOCA dose appearing in the Staff Safety Evaluation of the two stations, the total dose for thyroid was 140.8 rem for Quad-Cities and 111.9 rem for Dresden. These doses are well below the 10 CFR 100 regulation of 300 rem thyroid dose.

The second method of dose calculation consisted of the determination of the cumulative probability of exceeding a certain dose during a year, assuming that the accident has occurred every hour of the year and lasted for 30 days. This method is described in detail in Section A.4 of Appendix A. To this end, the code WINDOW,[25] developed by Pickard, Lowe and Associates, Inc., was employed.

The model for estimating the probability of an individual receiving an integrated dose in excess of a given amount resulting from the containment purging, utilizes long periods of hourly weather measurements to simulate sequences of atmospheric diffusion conditions over a given time period following the postulated accident. These sequences are coupled with a postulated accident which might occur at any random time. The WINDOW program computes the integrated off-site doses over a selected time period (or window). The processing begins for the selected window starting with the first hour of X/Q record being used and is then repeated for the same elapsed time period (window) starting a new integrating period with each subsequent hour of X/Q data. The processing continues for a total of up to 8760 hours, or for one year of data. In this process, an integrated dose over the given window has been computed and stored effectively assuming that an accident has occurred during each hour of the year. The window length selected for the purposes of this analysis is 720 hours. Assuming that there were 8760 integrated 720 hour doses for each location being investigated, the probability of an individual at any one of these locations receiving a given dose (or greater) is determined by dividing the total number of occurrences of each dose (or greater) at this location by the total number of integration periods. The total number of integration periods for this analysis is 8760 hours. The cumulative probability is computed by finding the total occurrences of doses equal to or in excess of sequentially smaller doses.

The results of this analysis show that the 5 percent probable doses for Dresden as well as Quad-Cities Stations are less than the doses resulting from the first method described above. Thus, the utilization of X/Q data given in Regulatory Guide 1.3[24] renders conservative results.

IV. CONCLUSIONS

The above analysis shows that a 2561 Mw(t) BWR can operate in compliance with the August 14, 1974 draft of Regulatory Guide 1.7 without an inerted containment. The results of the previous sections showed that by utilizing a highly feasible hydrogen control scheme to limit the concentration of hydrogen in the containment to below 4 v/o the total resulting dose, purging plus LOCA, was well below the 10 CFR 100 limits. It is concluded that the requirement for inerting the Dresden Station and Quad-Cities Station containments should be removed from their respective technical specifications.

V. REFERENCES

1. Regulatory Guide 1.7, "Control of Combustible Gas Concentrations in Containment Following a Loss of Coolant Accident" (Revised), April 5, 1974.

2. Regulatory Guide 1.7, "Control of Combustible Gas Concentrations in Containment Following a Loss of Coolant Accident" (Revised), August 14, 1974.

3. Title 10 - Energy, Code of Federal Regulations, Part 50 - "Licensing of Production and Utilization Facilities," Section 50.46 Acceptance Criteria for Emergency Core Cooling Systems for Light Water Nuclear Power Reactors, December 28, 1973.

4. Title 10 - Energy, Code of Federal Regulations, Part 100 - "Reactor Site Criteria," December 28, 1973.

5. L. W. Carlson, R. M. Knight and J. O. Henrie, "Flame and Detonation Initiation and Propagation in Various Hydrogen-Air Mixtures, With and Without Water Sprays," AI-73-29, May 11, 1973.

6. B. C. Slifer and T. G. Peterson "Hydrogen Flammability and Burning Characteristics in BWR Containments," NEDO-10812, April, 1973.

7. A. L. Furno, Thirteenth Symposium (International) on Combustion, 1971, p. 593.

8. Dresden Nuclear Power Station Unit 3 Safety Analysis Report, Amendment 23 - "Hydrogen Generation in a Boiling Water Reactor," Docket 50249-39, August 11, 1970.

9. K. V. Moore and W. H. Rettig, "RELAP4 - A Computer Program for Transient Thermal-Hydraulic Analysis," UC-32, December 1973.

10. D. R. Evans, "MOXY: A Digital Computer Code for Core Heat Transfer Analysis," IN-1392 August 1970.

11. R. W. Griebe, "MOXEI, A Computer Program for BWR Core Heat-Up Analysis," EI-Proprietary Code.

12. R. W. Griebe, K. D. Richert, M. E. Radd and C. M. Moser, "6KILER, Ver 001, A Digital Computer Code for BWR/6 Core Heat Transfer Analysis," EI 74-5, February 1974.

13. J. D. Duncan and J. E. Leonard, "Thermal Response and Cladding Performance of an Internally Pressurized, Zircaloy-Clad, Simulated BWR Fuel Bundle Cooled by Spray Under Loss-of-Coolant Conditions," GEAP-13112, April 1971.

14. R. L. Rittenhouse, D. O. Hobson, and R. D. Waddell, Jr., "The Effect of Light-Water Reactor Fuel Rod Failure on the Area Available for Emergency Coolant Flow Following a Loss-of-Coolant Accident," ORNL-4752, January 1972.

15. General Electric Company, "Core Flow Distribution in a Modern Boiling Water Reactor as Measured in Monticello," NEDO-10299, January 1971.

16. Commonwealth Edison Company, Dresden Nuclear Power Station Unit 3 Special Report No. 14, "Hydrogen Flammability Control System in a Boiling Water Reactor," May 1971.

17. Commonwealth Edison Company, "Quad-Cities Station Units 1 and 2 Final Safety Analysis Report," Docket 50-254 and 50-265.

18. Commonwealth Edison Company, "Dresden Nuclear Power Station Units 2 and 3 Safety Analysis Report," Docket 50-237 and 50-249.

19. ORNL Nuclear Safety Research and Development Program, Bimonthly Report, ORNL-TM-3212, September-October 1970.

20. ORNL Nuclear Safety Research and Development Program, Bimonthly Report, ORNL-TM-3411, March-April 1971.

21. ORNL Nuclear Safety Research and Development Program, Bimonthly Report, ORNL-TM-3342, January-February 1971.

22. Safety Evaluation, Division of Reactor Licensing USAEC, In the Matter of Commonwealth Edison Company Quad-Cities Station Units 1 and 2, Docket Numbers 50-254 and 50-265, August 25, 1971.

23. Safety Evaluation, Division of Reactor Licensing USAEC, In the Matter of Commonwealth Edison Company Dresden Station Units 2 and 3, Docket Numbers 50-237 and 50-249.

24. Regulatory Guide 1.3, "Assumptions Used for Evaluating the Potential Radiological Consequences of a Loss of Coolant Accident for Boiling Water Reactors," June 1974.

25. K. Woodard, "Probability Treatment of Atmospheric Dispersion for Dose Calculations," Nuclear Technology, Vol. 12, November 1971.

26. General Electric Company, "GEGAP-III: A Model for the Prediction of Pellet-Cladding Thermal Conductance in BWR Fuel Rods," NEDO-20181, November 1973.

APPENDIX A

ANALYTICAL MODELS AND CALCULATIONS

A.1 RELAP4

The RELAP4 model of the Quad Cities unit contains the essential details to describe the transient response of the system to a double-ended break in one of the recirculation loops upstream of the pump, pump suction, near the reactor vessel outlet. The model consists of 21 fluid volumes describing the primary system and a containment volume, along with 30 flow paths connecting the fluid volumes. Heat storage and conduction from the walls and internals are described by 27 heat slabs in addition to 6 active power generating regions for the nuclear core.

A.1.1 Fluid Volumes

The fluid control volumes, as shown in Figure A1, are described as follows:

The core outlet region (upper plenum) is combined with the cyclone steam separators into a single volume. The fluid leaving the separators enters the mixing plenum region where the separated steam flows into the dryers and the liquid flows into the downcomer. The steam dryers are combined with the upper steam dome into a single volume where the flow to turbines is described by an explicit time-dependent table. The downcomer region includes the feedwater injection region. Flow from the downcomer region feeds the two recirculation loops as well as the suction side to the jet pumps. Each recirculation loop is divided into control volumes describing the suction line, each pump, and the discharge line that drives the jet pumps. The jet pump drive lines from each recirculation loop header are grouped together to feed one jet pump and the 10 jet pumps to each recirculation loop are grouped together as a single effective jet pump and these two equivalent jet pumps thus feed the lower plenum. The core is divided into 7 regions; 3 axial hot bundles; 3 axial average regions; and a single bypass.

One-dimensional momentum flux effects are utilized in all flow paths.

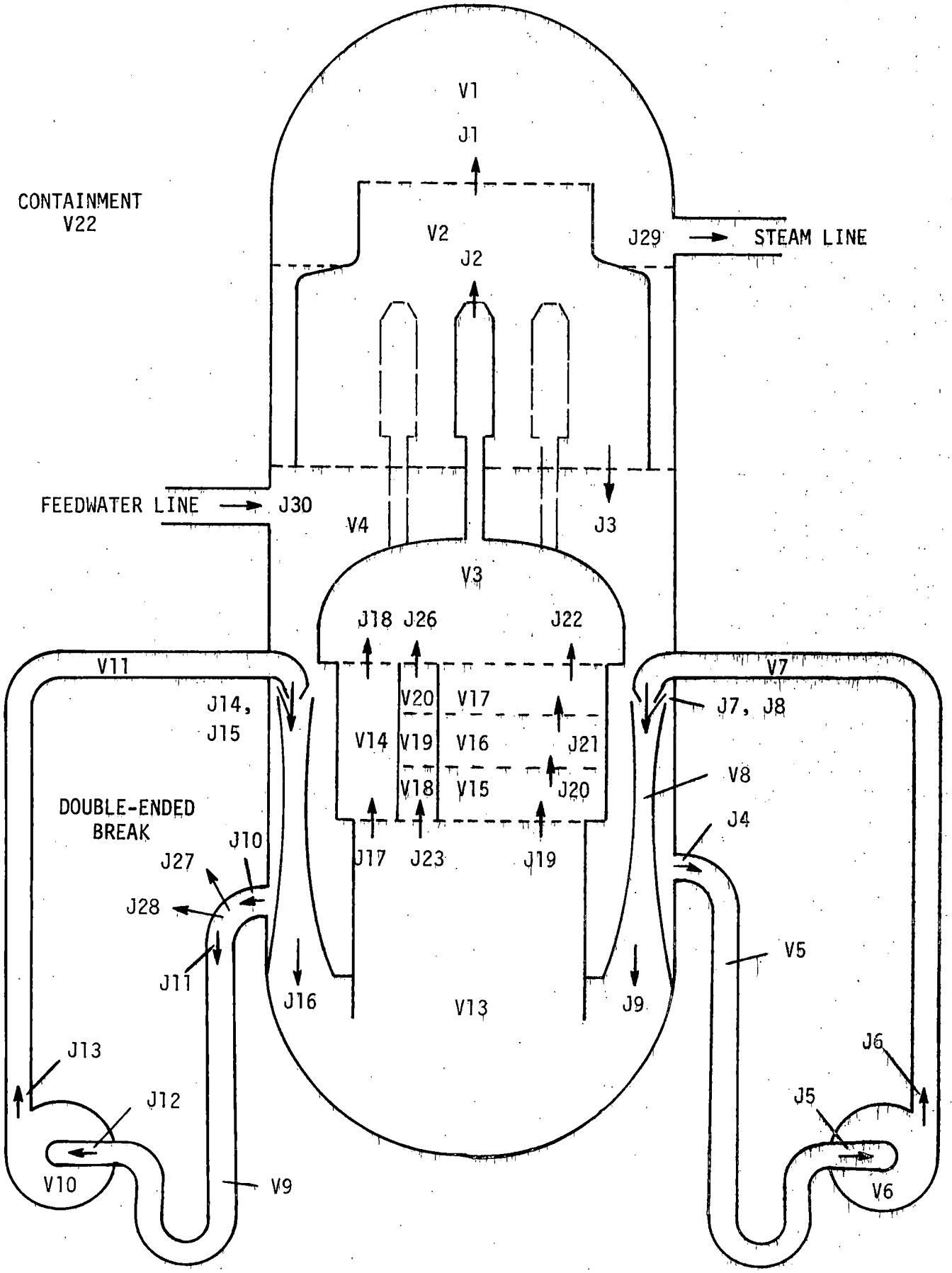

FIGURE A1 - RELAP4 GEOMETRIC MODEL

A.1.2 Passive Heat Storage

The stored energy in the various walls and internals is modeled for the components appropriate to each fluid control volume. These heat storage slabs are listed in Table A-1 and form either a conduction path between adjacent fluid volumes or act as a heat source within a single volume. Each equivalent slab represents the metal mass and fluid surface area of a combination of actual hardware appropriate to the particular fluid volume.

A.1.3 Pumps

The recirculating pumps are described by a set of homologous pump curves for normalized head and torque appropriate to a Byron-Jackson pump with a specific speed of N_s = 2700. The calculated pump head is degraded linearly with quality as the suction quality varies from 0 to 1 percent.

The jet pumps, 10 per recirculation loop, are modeled using the momentum exchange equations standard to RELAP 4. The 10 actual jet pumps per recirculation loop are modeled as one equivalent jet pump.

A.1.4 Control Actions

The model assumes that power to the recirculating and feedwater pumps fails at the initiation of the break. Steam line isolation valves close in 3.5 seconds and the feedwater coasts to a stop in 2.0 seconds.

The recirculating line break is implemented by closing an imaginary valve in the junction being severed and simultaneously opening a full pipe break area on both sides of the valve. This technique then describes a double ended break in the recirculation line near the position where the recirculation line bends downward from the vessel to the pump. Moody choking is used unless the break flow is calculated to be subsonic.

TABLE A-1

PASSIVE HEAT STORAGE SLABS

Slab Description	Material	Fluid Regions
Pressure Vessel	Carbon Steel with stainless Clad	Steam Dome
"	"	Mixing Plenum
"	"	Downcomer
"	"	Lower Plenum
Shroud	Stainless steel	Downcomer - Bypass
"	"	Downcomer - Upper plenum
"	"	Downcomer - Lower plenum
Recirc. Pipe	"	Unbroken suction
"	"	Unbroken discharge
"	"	Broken stub
"	"	Broken suction
"	"	Broken discharge
Pump Case	"	Unbroken loop
"	"	Broken loop
Jet Pump Case	"	Unbroken loop
"	"	Broken loop
Internals	"	Lower plenum
Internals	"	Downcomer
Core Outlet Tubes	"	Upper plenum - Downcomer
Internals	"	Dryer
Dryer Surfaces	"	Mixing plenum - Steam dome
Separator Surfaces	"	Upper plenum - Mixing plenum
Channel Boxes	Zirc	Lower core - Bypass
"	"	Middle core - Bypass
Channel Boxes	Zirc	Upper core - Bypass
Lower Grid Framework	Stainless Steel	Bypass - Lower plenum
Upper Grid Framework	"	Upper plenum - Bypass

A.1.5 Reactor Core

The reactor core is modeled with a single bypass region representing the fluid on the outside of the canisters. The heated core, except for one hot bundle, is modeled as 3 axial regions, and the remaining hot bundle is also modeled with 3 axial regions. The peaking factors are 1.57 axial and 1.27 radial. The initial power is 102 percent of the nominal rated power (2561 Mw(t)). All fuel is assumed to be the standard 7 X 7 arrays with a gap conductivity that varies with gap width. The initial conductivity is based on the minimum value of 500 BTU/hr-ft^2-°F for a 5.5 mil gap.

A.1.6 Reactor Power and Reactivity

Reactor power is calculated from a one-point neutron kinetic model with 6 delayed neutron groups, 11 equivalent decay heat groups yielding ANS + 20 percent and two equivalent actinide groups. The reactivity feedback includes core voiding, Doppler fuel temperature, and scram rods. Reactor scram begins 1.2 seconds after the break and the rods are fully inserted in an additional 2.3 seconds. All reactivity feedback is assumed to be generated in the average region.

A.2 MOXEI

The core heat-up calculation was performed by utilizing the output of the modified RELAP4 code. In the blowdown calculation, the core had been separated into three radial zones. The first zone was the hot zone representing the hot channel in the core which was that portion of the core having the highest radial peaking factor. The second radial zone represented the average core. Each of these two radial zones was separated into three axial zones for the blowdown calculation. The third radial zone was a single by-pass region.

In addition, two versions of the core heat-up code were used to do the calculation for the regions representing the core. The first of these has been described in the section which covers the addition of the rod ballooning and double metal-water reaction calculation. This version of the code was utilized to represent the three inch section of the core having the highest axial peaking factor and allowed rod ballooning and perforation. Another version of the code which did not allow rod ballooning and perforation was utilized to calculate the heat-up for all other axial locations in the core. Thus, it was possible to separate the core into the three axial regions having the power peaking profiles shown in Figure A-2. The axial peaking profile utilized for all the bundles considered that 20 percent of the core had an axial peaking factor of 1.57, 30 percent of the axial length had a peaking factor of 1.3, and 50 percent of the axial length had a peaking factor of 0.7. The choice of three axial peaking factors allowed for a significant portion of the core axial length to have the maximum linear heat generation rate. This resulted in an over-estimate of the core axial power by 5.4 percent during the heat-up calculations. In both the code versions utilized for the core heat-up calculation, the steady-state gap conductance value chosen was the minimum value presented in Figure A-3 which was taken from NEDO-20181.[26] This minimum gap conductance value was chosen to be conservative in that it represented the conditions which resulted in the highest stored energy within the fuel pellet at the time of accident initiation. Only the three inch section of the

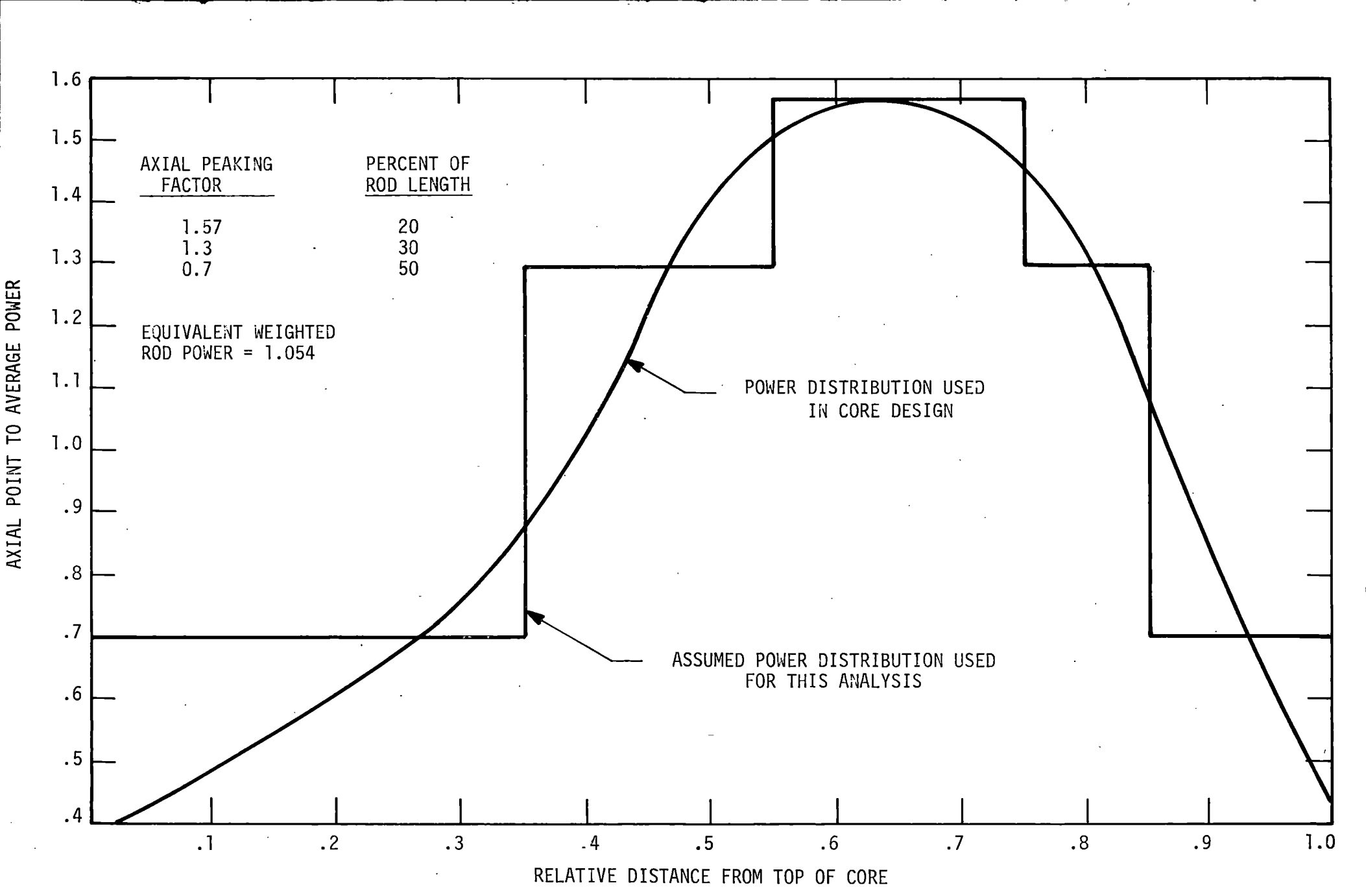

FIGURE A2 - DETERMINATION OF AXIAL PEAKING FACTORS AND CORRESPONDING PERCENTAGE OF CORE LENGTH

core which considered the rod ballooning and rupture was allowed to have a variable gap conductance. All of the other axial locations in the core were considered to have this minimum steady-state value which was taken from Figure A-3, and is shown in graphical form in Figure A-4. The local peaking factor distribution within all rod bundles of the core for the heat-up calculation is shown in Figure A-5.

Shown in Figure A-6 is a normalized plot of radial peaking factor as a function of the fraction of bundles greater than the indicated peaking factor. Figure A-6 shows both a typical distribution and the step-wise distributions used for the analysis. Thus a full 20 percent of the core was assumed to have the maximum radial peaking factor of 1.47, 80 percent was assumed to have a radial peaking factor of 1.1, and 30 percent to have a radial peaking factor of 0.8. Summation of the three radial peaking factors times the respective fraction of core yields an excess radial power generation factor of 8.4 percent for this analysis technique. Both the core overpower and the maximum radial peaking factor represent a conservative radial power distribution function.

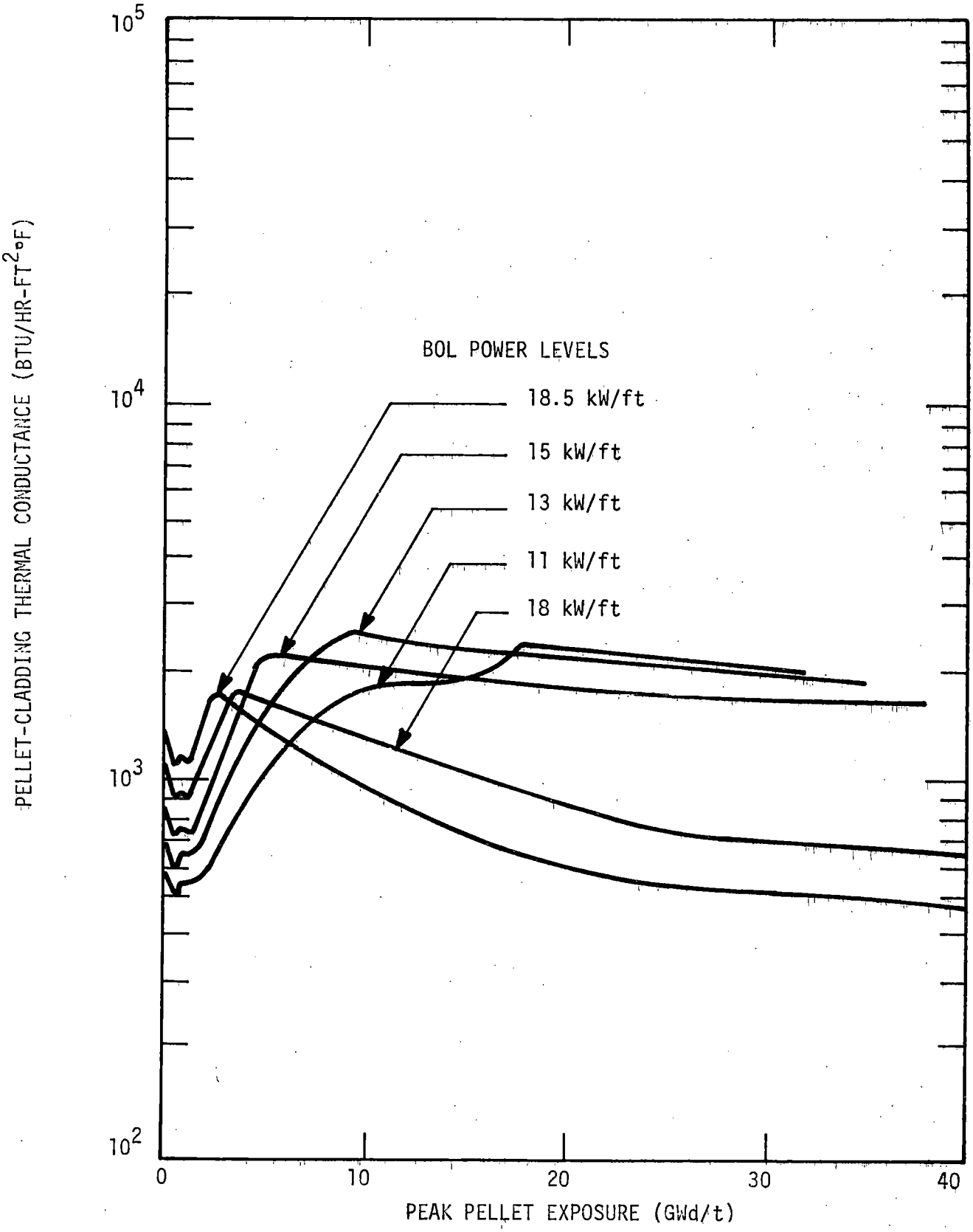

FIGURE A3 - GAP CONDUCTANCE FOR 7 X 7 FUEL IN A BWR/5 SYSTEM (FIGURE 4.3 OF NEDO-20181)[26]

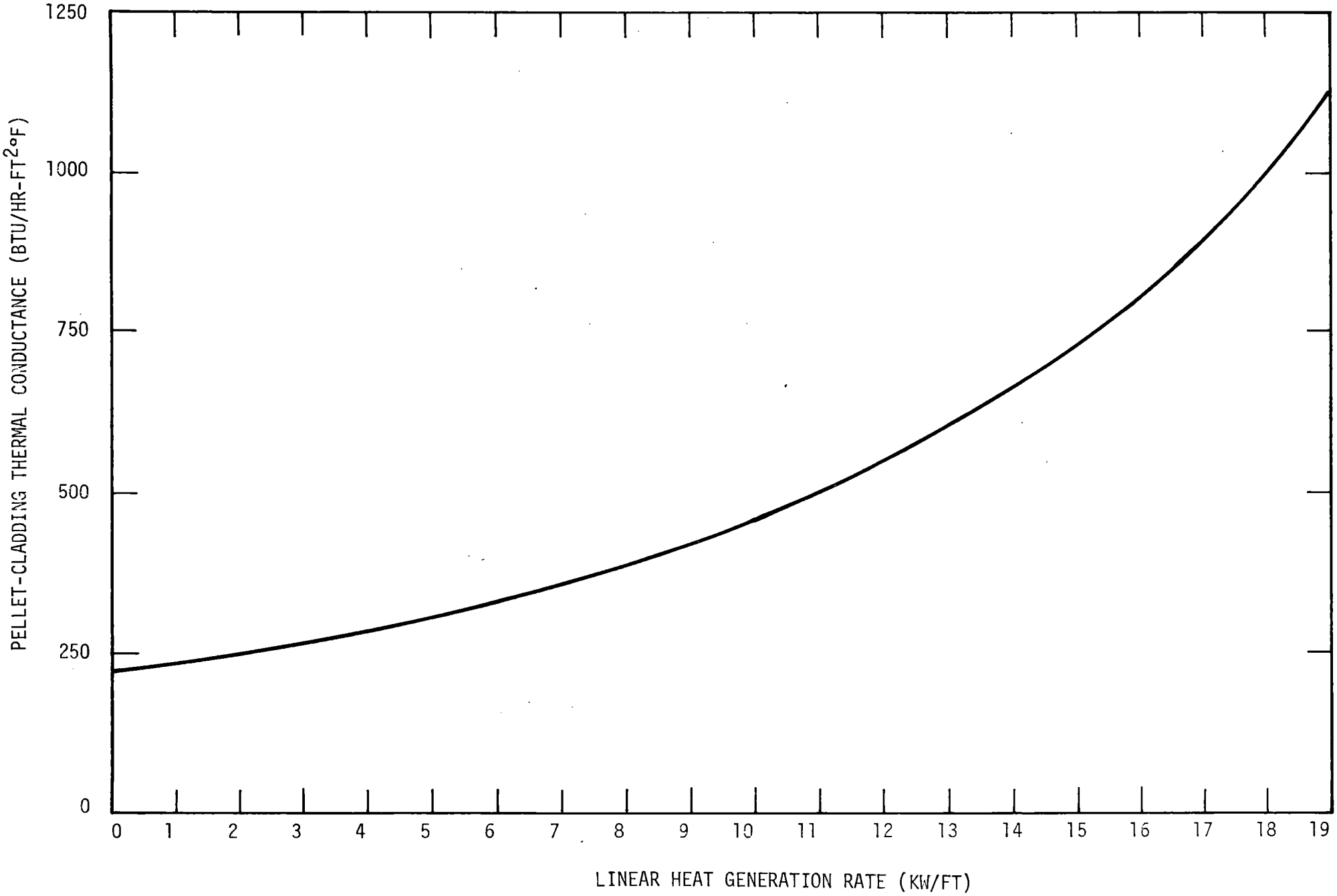

FIGURE A4 - MINIMUM GAP CONDUCTANCE VALUES TAKEN FROM Figure A5 OF THIS REPORT AND USED IN THIS ANALYSIS

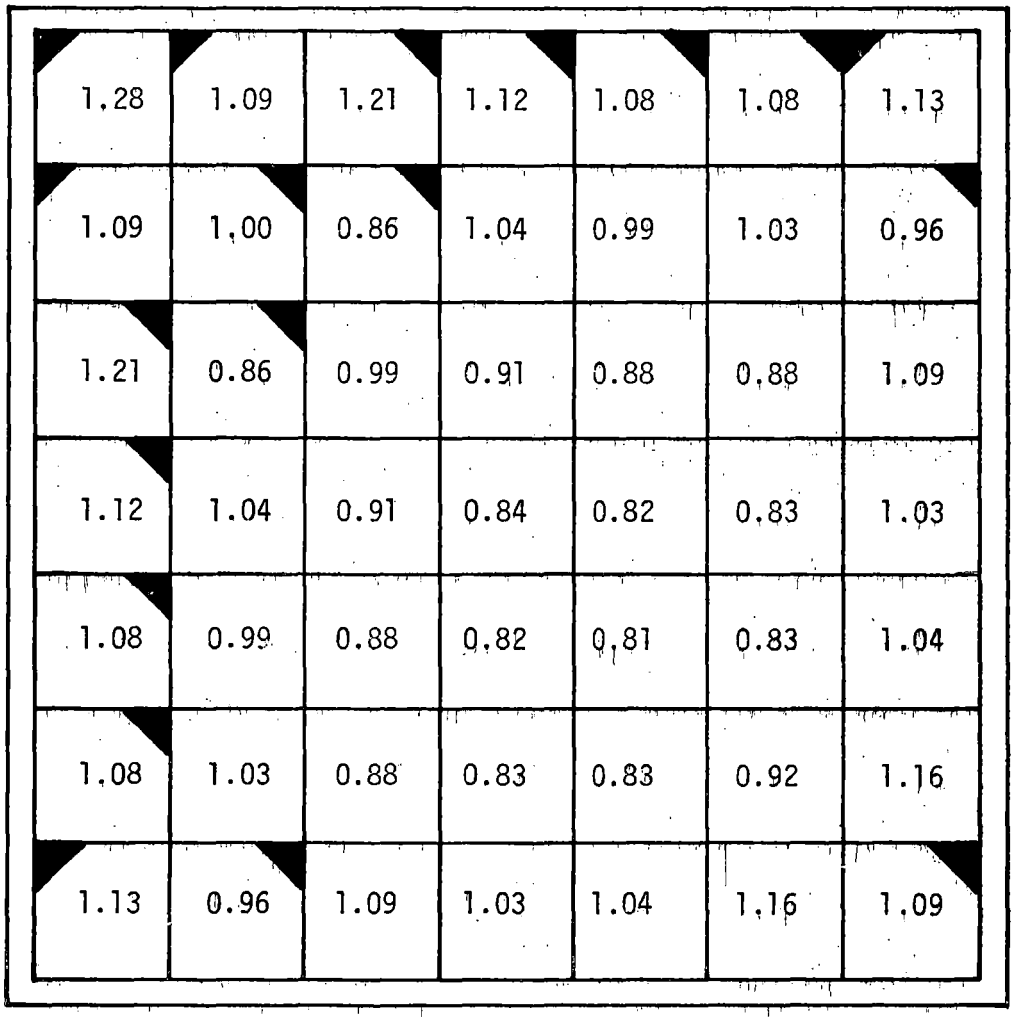

INITIAL ENRICHMENT

1.20 W/O U-235 (3 RODS)

1.69 W/O U-235 (16 RODS)

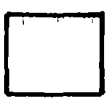

2.47 W/O U-235 (30 RODS)

FIGURE A5 - ASSUMED LOCAL POWER PEAKING FOR THIS ANALYSIS (FROM FIGURE 3.3.1 OF THE DRESDEN 2 and 3 FSAR) [18]

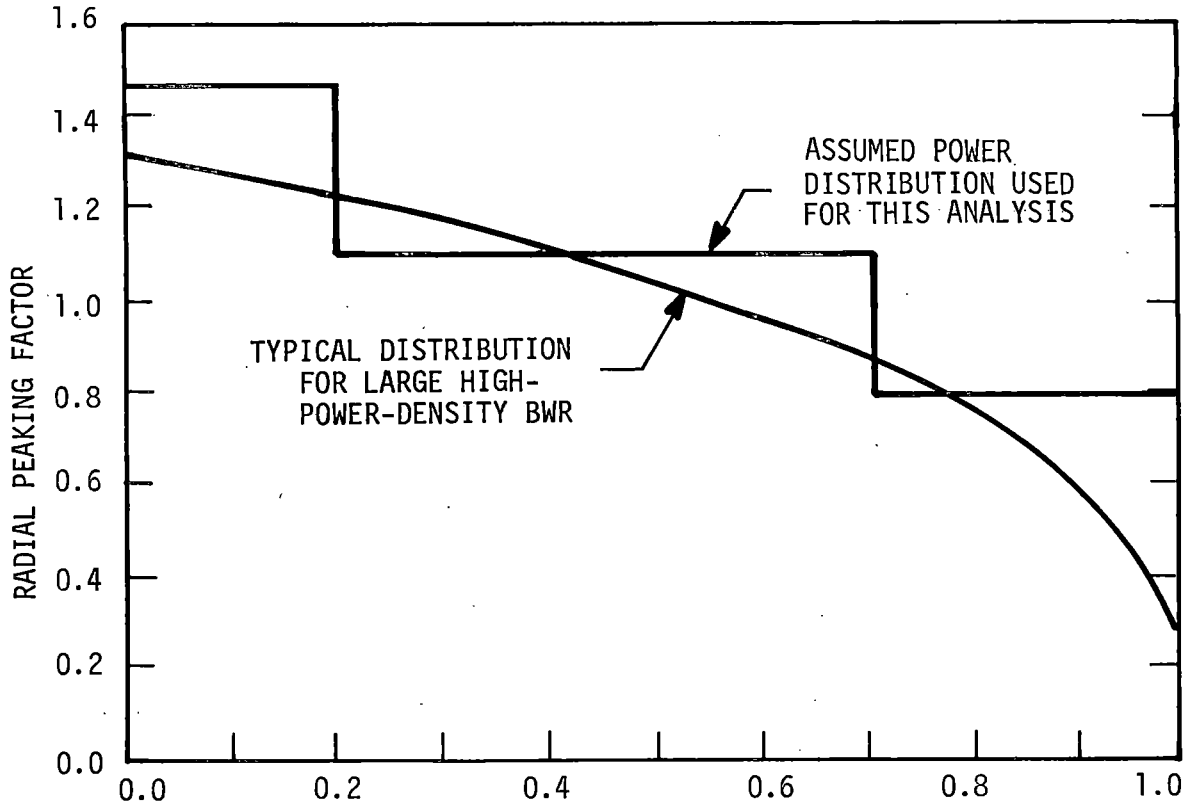

FIGURE A6 - RADIAL POWER DISTRIBUTION FOR A TYPICAL LARGE HIGH-POWER-DENSITY BWR

A.3 Hydrogen and Oxygen Generation Model

In calculating the concentrations of hydrogen and oxygen in the drywell and suppression pool, the conservative assumption is made that the two volumes are totally separate from each other. The interchange of masses between the two volumes which takes place during blowdown, and the period during which the vacuum breakers open, thus providing further dilution for the hydrogen, is neglected. Furthermore, the effect of water vapor dilution is conservatively unaccounted for. The equations describing the events in the drywell and the suppression pool are shown below:

Hydrogen Generation in the Drywell

$$\frac{P_1(t) + P_{2CH_2}(t)}{359 \times N_c(t)} - R_{C.L.}(t) \times C_{CH_2}(t) - \frac{R_{1env}}{359 \times N_c(t)} \times C_{CH_2}(t) - \frac{R_{2env}}{359 \times N_c(t)} \times C_{CH_2}(t) = \frac{dC_{CH_2}(t)}{dt}$$

Oxygen Generation in the Drywell

$$\frac{P_{2CO_2}(t)}{359 \times N_c(t)} - R_{C.L}(t) \times C_{CO_2} - \frac{R_{1env}}{359 \times N_c(t)} \times C_{CO_2}(t) + \frac{R_{2env} \times .21}{359 \times N_c(t)} - \frac{R_{2env}}{359 \times N_c(t)} \times C_{CO_2}(t) = \frac{dC_{CO_2}(t)}{dt}$$

and

$$\frac{dN_c(t)}{dt} = \frac{P_1(t) + P_{2CH_2}(t) + P_{2CO_2}(t)}{359} - R_{C.L}(t)\, N_c(t) - \frac{R_{1env}}{359} + \frac{R_{2env}}{359}$$

Hydrogen Generation in the Suppression Pool

$$\frac{P_{2S.P.H_2}(t)}{359 \times N_{S.P}(t)} - \frac{R_{1env}}{359 \times N_{S.P}(t)} \times C_{S.P.H_2}(t)$$

$$- \frac{R_{2env}}{359 \times N_{S.P}(t)} \times C_{S.P.H_2}(t) = \frac{dC_{S.P.H_2}(t)}{dt}$$

Oxygen Generation in the Suppression Pool

$$\frac{P_{2S.P.O_2}(t)}{359 \times N_{S.P}(t)} - \frac{R_{1env}}{359 \times N_{S.P}(t)} \times C_{S.P.O_2}(t) + \frac{R_{2env} \times .21}{359 \times N_{S.P}(t)}$$

$$- \frac{R_{2env}}{359 \times N_{S.P}(t)} \times C_{S.P.O_2}(t) = \frac{dC_{S.P.O_2}(t)}{dt}$$

and

$$\frac{dN_{S.P}(t)}{dt} = \frac{P_{2S.P.H_2} + P_{2S.P.O_2}}{359} - \frac{R_{1env}}{359} + \frac{R_{2env}}{359}$$

where: $P_1(t)$ is the hydrogen yield from metal-water reaction, SCFM

$P_{2CH_2}(t)$ is the radiolytic hydrogen generation rate in the drywell, SCFM

$P_{2CO_2}(t)$ is the radiolytic oxygen generation rate in the drywell, SCFM

$P_{2S.P.H_2}(t)$ is the radiolytic hydrogen generation rate in the suppression pool

$P_{2S.P.O_2}(t)$ is the radiolytic oxygen generation in the suppression pool

$R_{C.L.}(t)$ is drywell leakage, fraction of total moles/min,

R_{1env} is the purge rate, SCFM

R_{2env} is the make up rate, SCFM

$C_{CH_2}(t)$ is the hydrogen concentration in the drywell

$C_{CO_2}(t)$ is the oxygen concentration in the drywell

$C_{S.P.H_2}(t)$ is the hydrogen concentration in the suppression pool

$C_{S.P.O_2}(t)$ is the oxygen concentration in the suppression pool

$N_c(t)$ is the total moles of gas in the drywell

$N_{S.P}(t)$ is the total moles of gas in the suppression pool

359 is the number of cubic feet per lb. mole of gas at 14.7 psi and 32°F

The calculation is performed by converting the above equations into a finite difference form. It is assumed initially that the number of moles, $N_c(0)$ and $N_{S.P}(0)$ are obtained from drywell and suppression pool initial conditions of 16.5 psi and 135°F and 95°F respectively. Moreover, $N_c(0)$ is increased by 2/3 moles since primary leakage into the drywell is assumed (see Section III). As the hydrogen and oxygen are produced and as long as $R_{1env} << R_{2env}$, the total moles in the drywell and suppression pool will increase and, consequently, the corresponding pressures will increase. It is also assumed that any temperature rise in the two volumes would be slight and thus have little effect on the pressures. To calculate the pressures the ideal gas laws are applied:

$$P_c(t) = \frac{N_c(t)\ R\ T_c}{V_c} \qquad P_{S.P}(t) = \frac{N_{S.P}(t)\ R\ T_{S.P}}{V_{S.P}}$$

where: $P_c(t)$ is the drywell pressure

$P_{S.P.}(t)$ is the suppression pool pressure

$N_c(t)$ is previously defined

$N_{S.P.}(t)$ is previously defined

R is the specific gas constants = 1545 $\left(\frac{\text{ft lb}_f}{\text{mole } ^\circ R}\right)$

T_c is the drywell temperature $\sim$ 135°F

$T_{S.P.}$ is the suppression pool temperature $\sim$ 95°F

V_c is the drywell free volume

$V_{S.P.}$ is the suppression pool free volume.

For the proposed method of hydrogen control R_{1env} is set equal to zero and R_{2env} is started by a high hydrogen concentration in the drywell. With R_{1env} set equal to zero and R_{2env} set at a certain rate, outside air would be admitted into the drywell and suppression pool thus slowly pressurizing them. Normally, this dilution would decrease the concentration in the drywell and suppression pool before the pressure in the two volumes reaches a certain level. Thus, R_{2env} would be stopped by a low hydrogen concentration in the drywell. However, after several initiations of R_{2env} it is possible that the pressure in the drywell or in the suppression pool would reach 50 percent of their design pressure. Whether it is in the drywell or in the suppression pool that the pressure reaches that setpoint, R_{2env} stops and R_{1env} is simultaneously started at a set rate. R_{1env} continues at that rate until the pressure in the drywell or suppression pool drops to a certain value, whichever happens later. At that time, R_{1env} stops and R_{2env} starts at its previous rate if the hydrogen concentration in the drywell is above the high concentration setpoint. It should be pointed out that the pressures in

the drywell and the suppression pool would be equalized through the downcomers or the vacuum breakers depending which way the pressure differential would be. This effect is conservatively neglected in this calculation. The hydrogen and oxygen concentrations in the drywell and suppression pool, their respective pressures and the times at which R_{1env} and R_{2env} start and stop, will be obtained as output. The entire accident is assumed to last for 30 days or 43,200 minutes.

A.4 Purging Model

It is assumed that 25 percent of the equilibrium radioactive iodine inventory developed from maximum full power operation of the core is available for leakage from primary reactor containment. 91 percent of this inventory was assumed to be in the form of elemental iodine, 5 percent of this inventory was assumed to be in the form of particulate iodine and 4 percent of this inventory was assumed to be in the form of organic iodides. Furthermore, 100 percent of the equilibrium radioactive noble gas inventory developed from maximum full power operation of the core was assumed to be immediately available for leakage from the reactor containment. The effect of radiological decay during holdup in the containment was taken into account. The equation describing the concentration of the nth isotope in the volume composed of the drywell and suppression pool is given by:

$$\frac{dA_n(t)}{dt} = -R_{C.L}(t) \times A_n(t) - \frac{2\ R_{lenv}}{(N_c(t) + N_{S.P}(t)) \times 359} \times A_n(t) - \lambda A_n(t)$$

and

$$C_n(t) = \frac{A_n(t)}{(N_c(t) + N_{S.P}(t)) \times 359 \times 28320}$$

where: A_n is the Curies of nth isotope available for leakage from containment
C_n is the concentration of the nth isotope, Ci/cc
λ_n is the decay constant for the nth isotope in min^{-1}
$N_c(t)$ and $N_{sp}(t)$ were previously defined
359 is a conversion factor from moles to ft^3 at 14.7 psi and 32°F
28320 is a conversion factor from ft^3 to cm^3.

Each time step the purge system, R_{lenv}, comes on, the total amount of activity per isotope released during that time step of purge operation is given by:

$$Rel_n = 2\ R_{lenv} \times 28320 \times C_n(t)\ \Delta t$$

For purposes of dose calculations, it is necessary to know the quantity of each radioactive material released during each hour after the accident, thus,

$$Rel_{n_i} = \int_{t_2}^{t_1} 2\ R_{lenv} \times 28320 \times C_n(t)\ dt$$

where t_1 goes from 1 - 2160 hour
t_2 goes from 0 - 2159 hour
i is the 1st, 2nd, 3rd. . . . .2160th hour of accident

Having computed the hourly amount of activity per isotope released into the Standby Gas Treatment System, the thyroid and whole body doses are computed next. The thyroid dose is computed by:

$$D_I = \sum_{n=1}^{4} (X/Q_i) \times BR \times [Rel_{n_i} \times (\alpha_o \times F_{nro} + \alpha_e \times F_{nre} + \alpha_p \times F_{nrp}] \times DCF_n$$

X/Q	atmospheric dispersion (sec/m^3)
BR	is the breathing rate (2.32×10^{-4} m^3/sec)
DCF_n	is a dose conversion factor, rem/Ci
D_i	incremental thyroid dose (rem) during the hour
α_o	is the organic fraction of initial iodine
α_p	is the particulate fraction of initial iodine
α_e	is the elemental fraction of initial iodine
F_{nro}	is the filter non removal fraction of organic iodine
F_{nrp}	is the filter non removal fraction of particulate iodine
F_{nre}	is the filter non removal fraction of elemental iodine